



## **Demography or selection on linked cultural traits or genes? Investigating the driver of low mtDNA diversity in the sperm whale using complementary mitochondrial and nuclear genome analyses**

Morin, Phillip; Foote, Andrew; Baker, C. Scott; Hancock-Hanser, Brittany; Kaschner, Kristin; Mate, Bruce; Mesnick, Sarah; Pease, Victoria; Rosel, Patricia; Alexander, Alana

### **Molecular Ecology**

DOI:

[10.1111/mec.14698](https://doi.org/10.1111/mec.14698)

Published: 01/06/2018

Peer reviewed version

[Cyswllt i'r cyhoeddiad / Link to publication](#)

*Dyfyniad o'r fersiwn a gyhoeddwyd / Citation for published version (APA):*

Morin, P., Foote, A., Baker, C. S., Hancock-Hanser, B., Kaschner, K., Mate, B., Mesnick, S., Pease, V., Rosel, P., & Alexander, A. (2018). Demography or selection on linked cultural traits or genes? Investigating the driver of low mtDNA diversity in the sperm whale using complementary mitochondrial and nuclear genome analyses. *Molecular Ecology*, 27(11), 2604-2619. <https://doi.org/10.1111/mec.14698>

#### **Hawliau Cyffredinol / General rights**

Copyright and moral rights for the publications made accessible in the public portal are retained by the authors and/or other copyright owners and it is a condition of accessing publications that users recognise and abide by the legal requirements associated with these rights.

- Users may download and print one copy of any publication from the public portal for the purpose of private study or research.
- You may not further distribute the material or use it for any profit-making activity or commercial gain
- You may freely distribute the URL identifying the publication in the public portal ?

#### **Take down policy**

If you believe that this document breaches copyright please contact us providing details, and we will remove access to the work immediately and investigate your claim.

1 Demography or selection on linked cultural traits or genes? Investigating the driver of  
2 low mtDNA diversity in the sperm whale using complementary mitochondrial and  
3 nuclear genome analyses

4

5 Phillip A. Morin<sup>1\*</sup>, Andrew D. Foote<sup>2</sup>, C. Scott Baker<sup>3,4</sup>, Brittany L. Hancock-Hanser<sup>1</sup>,  
6 Kristin Kaschner<sup>5</sup>, Bruce R. Mate<sup>3,4</sup>, Sarah L. Mesnick<sup>1</sup>, Victoria L. Pease<sup>1</sup>, Patricia E.  
7 Rosel<sup>6</sup>, Alana Alexander<sup>7,8</sup>

8

9 <sup>1</sup>Southwest Fisheries Science Center, National Marine Fisheries Service, National  
10 Oceanic and Atmospheric Administration, La Jolla, California, USA

11

12 <sup>2</sup>Molecular Ecology and Fisheries Genetics Laboratory, School of Biological Sciences,  
13 Bangor University, Bangor, Gwynedd, LL57 2UW, UK

14

15 <sup>3</sup>Marine Mammal Institute, Hatfield Marine Science Center, Oregon State University,  
16 2030 SE Marine Science Drive, Newport, OR 97365, USA,

17

18 <sup>4</sup>Department of Fisheries and Wildlife, College of Agricultural Sciences, 104 Nash Hall,  
19 Corvallis, OR 97330, USA

20

21 <sup>5</sup>Department of Biometry and Environmental System Analysis, Albert-Ludwigs-  
22 University of Freiburg, Tennenbacher Strasse 4, 79106 Freiburg, Germany

23

24 <sup>6</sup>Southeast Fisheries Science Center, National Marine Fisheries Service, National  
25 Oceanic and Atmospheric Administration, Lafayette, Louisiana, USA

26

27 <sup>7</sup>Biodiversity Institute, University of Kansas, 1345 Jayhawk Blvd, Lawrence, KS 66045,  
28 USA

29

30 <sup>8</sup>Current address: Department of Anatomy, University of Otago, Dunedin 9016, New  
31 Zealand

32

33 \*Corresponding author: [phillip.morin@noaa.gov](mailto:phillip.morin@noaa.gov)

34 Short title: Global phylogeography of the sperm whale

35 Keywords: cetacean, PSMC, population structure, Pleistocene

36

37 **Abstract**

38 Mitochondrial DNA has been heavily utilized in phylogeography studies for several  
39 decades. However, underlying patterns of demography and phylogeography may be  
40 misrepresented due to coalescence stochasticity, selection, variation in mutation  
41 rates, and cultural hitchhiking (linkage of genetic variation to culturally transmitted  
42 traits affecting fitness). Cultural hitchhiking has been suggested as an explanation  
43 for low genetic diversity in species with strong social structures, counteracting even  
44 high mobility, abundance and limited barriers to dispersal. One such species is the  
45 sperm whale, which shows very limited phylogeographic structure and low mtDNA  
46 diversity despite a worldwide distribution and large population. Here, we use  
47 analyses of 175 globally distributed mitogenomes and three nuclear genomes to  
48 evaluate hypotheses of a population bottleneck/expansion versus a selective sweep  
49 due to cultural-hitchhiking or selection on mtDNA as the mechanism contributing to  
50 low worldwide mitochondrial diversity in sperm whales. In contrast to mtDNA  
51 control region (CR) data, mitogenome haplotypes are largely ocean-specific, with  
52 only one of 80 shared between the Atlantic and Pacific. Demographic analyses of  
53 nuclear genomes suggest low mtDNA diversity is consistent with a global reduction  
54 in population size that ended approximately 125,000 years ago, correlated with the  
55 Eemian interglacial. Phylogeographic analysis suggests that extant sperm whales  
56 descend from maternal lineages endemic to the Pacific during the period of reduced  
57 abundance, and have subsequently colonized the Atlantic several times. Results  
58 highlight the apparent impact of past climate change, and suggest selection and  
59 hitchhiking are not the sole processes responsible for low mtDNA diversity in this  
60 highly social species.

61

## 62 **Introduction**

63 There is a growing body of literature indicating that the commonly held tenet of  
64 population genetics, that genetic diversity should be correlated with population size, is  
65 often violated, particularly for mitochondrial DNA (mtDNA) (Bazin *et al.* 2006). When  
66 mtDNA diversity is found to be low in currently abundant populations, several  
67 hypotheses have been invoked to explain the discord, including population bottlenecks  
68 (e.g., Hoelzel *et al.* 2002; O'Brien 1994), selection on mtDNA (e.g., Finch *et al.* 2014;  
69 Foote *et al.* 2011), variation in mutation rates (Lyrholm *et al.* 1996), and cultural  
70 hitchhiking (linkage of genetic variation to culturally transmitted traits affecting fitness;  
71 Kopps *et al.* 2014; Premo & Hublin 2009; Whitehead 1998, 2005).

72  
73 Among globally distributed large whales, most baleen whales exhibit high mtDNA  
74 diversity relative to toothed whales and are divided into multiple subspecies and  
75 genetically distinct populations (e.g., fin, humpback, gray and blue whales; Archer *et al.*  
76 2013; Baker *et al.* 2013; Jackson *et al.* 2014; Lang *et al.* 2014; Leduc *et al.* 2016).  
77 Among toothed whales, however, unusually low mitochondrial DNA (mtDNA) diversity  
78 in some of the social odontocetes (e.g., sperm, pilot, killer, and false-killer whales;  
79 Alexander *et al.* 2016; Alexander *et al.* 2013; Hoelzel *et al.* 2002; Martien *et al.* 2014;  
80 Van Cise *et al.* 2016) has limited power to infer population structure, phylogeography  
81 and historical demography using traditional genetic tools. The sperm whale (*Physeter*  
82 *macrocephalus*) is particularly enigmatic in this respect, as it is one of the most  
83 cosmopolitan and abundant of the large odontocetes, and known to move over large  
84 ranges of up to thousands of kilometers over annual or longer time periods (Mizroch &  
85 Rice 2013; Steiner *et al.* 2012; Straley *et al.* 2014), yet it exhibits low mtDNA diversity  
86 and evidence of female philopatry (Alexander *et al.* 2016; Lyrholm & Gyllensten 1998;  
87 Lyrholm *et al.* 1999; Mesnick *et al.* 2011).

88  
89 In addition to the sperm whale's broad distribution throughout the world's oceans, it is  
90 considered relatively abundant even post-industrial whaling, with the global population  
91 size estimated in 2002 at 360,000, approximately 1/3 of its pre-whaling population size  
92 (Whitehead 2002). Previous genetic studies based on mtDNA control region (CR)

93 sequences showed haplotype frequency differences among oceans, major within-ocean  
94 geographic regions and female-led social groups, but limited phylogeographic signal,  
95 largely due to the low CR diversity and occurrence of three common haplotypes in all  
96 large ocean basins (Alexander *et al.* 2016; Engelhaupt *et al.* 2009; Lyrholm & Gyllensten  
97 1998; Mesnick *et al.* 2011; Whitehead 1998).

98

99 In other species with low levels of CR diversity, complete mitochondrial genome  
100 (mitogenome) sequences have been used to detect phylogeographic structure and estimate  
101 divergence times and historical demography with higher precision (e.g., Archer *et al.*  
102 2013; Buddhakosai *et al.* 2016; Morin *et al.* 2010; Morin *et al.* 2015; Shamblin *et al.*  
103 2012). Several hypotheses have been proposed to explain the extremely low mtDNA  
104 diversity in sperm whales, including a population bottleneck (Lyrholm & Gyllensten  
105 1998; Lyrholm *et al.* 1996), low mutation rate (Lyrholm *et al.* 1996; Whitehead 1998),  
106 stochastic variation in maternal lineage survival (Amos 1999; Tiedemann & Milinkovitch  
107 1999), cultural hitchhiking (Whitehead 1998, 2005; Whitehead *et al.* 2017), and selective  
108 constraints on CR sequences that limit accumulation of variation and lead to saturation of  
109 sites free to vary (Alexander *et al.* 2013). Alexander *et al.* (2013) used complete  
110 mitogenome sequences (N=17) to evaluate support for some of these hypotheses, and  
111 concluded that the data were consistent with a bottleneck or selective sweep (involving  
112 selection on mitochondrial protein-coding regions or cultural hitchhiking), and found no  
113 evidence for selective constraint on the control region or slow substitution rates in sperm  
114 whale mtDNA relative to other cetaceans. In this study, we analyze complete  
115 mitogenomes from 175 globally distributed sperm whale samples to investigate  
116 phylogeography, selection, and historical demography. We compare demographic  
117 inferences from mitogenomes and nuclear genomes to evaluate the previously proposed  
118 hypotheses of a population bottleneck/expansion versus a selective sweep due to cultural-  
119 hitchhiking or selection on mtDNA as the mechanism contributing to low worldwide  
120 mitochondrial diversity in sperm whales.

121

## 122 **Materials and Methods**

123 *DNA extraction and library preparation*

124 Sperm whale tissue samples (n=158) collected by live-biopsy or from dead stranded  
125 animals were stored in salt-saturated 20% DMSO at -20°C in the US National Marine  
126 Fisheries Service (NMFS) Marine Mammal and Sea Turtle Research (MMASTR)  
127 Collection at the Southwest Fisheries Science Center (SWFSC), or in 70% ethanol at -  
128 20°C at the Oregon State University Cetacean Conservation and Genomics Laboratory  
129 (CCGL). Sample information is in supplemental Table S1. DNA from SWFSC samples  
130 was extracted from tissue samples using either a silica-membrane method (Qiaextractor®  
131 DX reagents, Qiagen, Valencia, CA, USA) or a simple salt-precipitation procedure  
132 (Miller *et al.* 1988). DNA libraries for these samples were constructed and enriched for  
133 mitochondrial DNA according to Hancock-Hanser *et al.* (2013), and sequenced in 3 pools  
134 of 49-66 samples with Illumina GEII, HiSeq (100 bp) and NextSeq (75 bp) single-end  
135 reads. Eleven samples were repeated in two pools to increase read depth of coverage.  
136 CCGL samples were extracted using a standard phenol/chloroform method (Sambrook *et*  
137 *al.* 1989), modified for smaller samples (Baker *et al.* 1994). Libraries for these samples  
138 were constructed from long-range PCR products following Alexander *et al.* (2013),  
139 individually-barcoded and prepared for sequencing using a Nextera XT DNA Sample  
140 Preparation Kit (Illumina, La Jolla, CA, USA). Sample libraries were pooled and  
141 sequenced in three Illumina MiSeq paired-end runs (two 250 bp, one 75 bp).

142

#### 143 *Sequence read quality control and assembly*

144 Assembly of sequence reads to the reference mitogenome (KC312603) was performed  
145 using custom scripts in R (R Core Team 2014) and publicly available programs as  
146 previously described (Hancock-Hanser *et al.* 2013; Dryad data repository doi:  
147 10.5061/dryad.cv35b). The reference mitogenome was modified to improve assembly  
148 coverage at the ‘ends’ of the linearized mitogenome by adding 40 bp from each end of  
149 the sequence to the opposite end (so that reads could map across the artificial break point  
150 of the linearized sequence). Nucleotide sites in the consensus sequence for each sample  
151 were called “N” if there were <3 reads, <9 reads where there was nucleotide variation at  
152 the site among reads, or >9 reads where a single nucleotide did not represent >70% of the  
153 reads. All sequences were aligned and visually inspected in the program GENEIOUS (V.  
154 6.0.5, Biomatters, Auckland, New Zealand), with indels and unique variants identified in

155 GENEIOUS then verified by visual inspection of the read alignments of individual  
156 sample assemblies in the BAM files. New and 17 previously published sequences  
157 (Alexander *et al.* 2013) were aligned and checked for frame-shift indels and coding  
158 sequence start and stop codons within protein-coding regions, based on published  
159 annotation of the reference sperm whale mitogenome.

160

#### 161 *Genetic diversity analyses and diagnosability*

162 The R package strataG (Archer *et al.* 2017a) was used to calculate haplotype and  
163 nucleotide diversity by geographically-defined population (stratum). To test if haplotypic  
164 diversity and nucleotide diversity within strata were significantly different from one  
165 another, we estimated the variance of each measure via a stratified bootstrap  
166 (supplemental methods). In each iteration of the bootstrap, individuals were randomly  
167 chosen with replacement from each stratum, with sample sizes determined by the  
168 empirical data set. At each of the 1000 bootstrap replicates, differences in nucleotide and  
169 haplotype diversity were calculated between each stratum (stratum 1 diversity - stratum 2  
170 diversity, for each measurement). Strata were considered to have significantly different  
171 haplotype and/or nucleotide diversity if the observed difference was in the lower 5% of  
172 the distribution (strata 2 significantly greater diversity than stratum 1), or in the upper 5%  
173 of the distribution (strata 1 significantly greater than stratum 2).

174

175 Diagnosability is a measure of the ability to correctly determine whether a specimen of  
176 unknown origin can be correctly assigned to a group based on a trait or traits (Archer *et al.*  
177 *al.* 2017b). To test the diagnosability of mitogenome sequences between Atlantic and  
178 Pacific sperm whales, we conducted a Random Forest analysis (Breiman 2001) to create  
179 a model to classify samples to ocean basins following Archer *et al.* (2017b). The Random  
180 Forest was built with 50,000 trees. Each tree was built using a random draw of 25  
181 samples (half of the smallest oceanic sample size of  $n = 50$  for the Atlantic, including the  
182 Gulf of Mexico and Mediterranean Sea) from each ocean basin to avoid biasing the  
183 model due to differences in sample size. The upper and lower confidence intervals of the  
184 correct classification score as well as the expected classification score (prior) were  
185 calculated as described in Archer *et al.* (2017b).

186

187 *Phylogenetic analyses*

188 Time-calibrated phylogenetic analysis was performed using two methods: creating a prior  
189 distribution for the time to most recent ancestor (TMRCA) using a two-phase process  
190 (described below), and estimating the TMRCA using previously published substitution  
191 rates (see *Demographic reconstruction* section). The two-phase method utilized BEAST  
192 (v 1.8; Drummond *et al.* 2012). Aligned coding sequences were extracted based on  
193 published start/stop codons of the reference sequence. Optimal substitution models for  
194 individual loci were determined based on Bayesian Information Content (BIC) using  
195 PartitionFinder (v 1.1.1; Lanfear *et al.* 2012). All loci were constrained to having the  
196 same underlying topology and clock rate (as loci on the mtDNA are fully linked without  
197 recombination). Phase 1 estimated the TMRCA for all sperm whale mitogenomes based  
198 on the coding partitions from four sperm whale haplotypes (mtGen11, 22, 30, 47)  
199 selected to represent the four major clades identified in a maximum likelihood tree of all  
200 full mitogenome unique haplotypes (PhyML v. 2.2.0; Guindon *et al.* 2009, implemented  
201 in Geneious), along with aligned coding region sequences from the pygmy sperm whale  
202 (*Kogia breviceps*, accession No. NC005272) and four beaked whale species (*Berardius*  
203 *bairdii*, NC005274; *Ziphius cavirostris*, KC776696; *Mesoplodon densirostris*,  
204 KF032860; *Hyperodon ampulatus*, NC005273). The Bayesian phylogeny was calibrated  
205 using lognormal distributions on two calibration nodes: Odontoceti (34.67 Myr: 95% CI  
206 29.93 – 40.17 Myr) (McGowen *et al.* 2009) and Ziphiidae (22 Myr: 14.86 – 32.56 Myr)  
207 (Dornburg *et al.* 2012; McGowen *et al.* 2009). The uclD prior was set to a uniform  
208 distribution (min. 1E-6, max. 1), the tree prior was speciation, Yule process, and the  
209 chain was 100M MCMC steps, logged every 10k steps. Convergence of two replicates  
210 and mixing were checked using TRACER (v1.5; Rambaut *et al.* 2014) and RWTY  
211 (Warren *et al.* 2017a). The maximum clade credibility tree was generated with  
212 TreeAnnotator (v1.8.1) in the BEAST software cluster (Drummond *et al.* 2012) after  
213 removal of the first 10% of trees.

214

215 The phylogenetic analysis of all sperm whale mitogenomes (Phase II) was conducted as  
216 above, separately for all complete mitogenome unique haplotypes (N=80) and unique

217 haplotypes of concatenated coding loci (N=60), with TMRCA calibration based on the  
218 lognormal distribution ( $\log(\text{stdev} = 0.2)$ ) of the median TMRCA estimate of sperm  
219 whales from Phase I (136.7 thousand years ago (KYA), 95% CI 85.2 – 201.1 KYA)  
220 following previously described methods (Morin *et al.* 2010; Morin *et al.* 2015). A strict  
221 clock was used with a constant size coalescent tree model. 100M MCMC steps and a  
222 single mutation model (TN93), selected based on the AIC in jModeltest v2.1 (Darriba *et al.*  
223 *al.* 2012), were used for the full-length mitogenome sequences. For the concatenated  
224 protein coding loci, we used 10M MCMC steps and 3<sup>rd</sup> position sites only, with two  
225 mutation models applied to *NADH6* and all other genes combined (HKY and TrN,  
226 respectively), based on analysis of individual loci in PartitionFinder. For both analyses,  
227 convergence was checked based on four replicate runs using TRACER v1.5 and RWTY.  
228

229 A haplotype median joining network (MJN: Bandelt *et al.* 1999) was created using the  
230 program POPART (Leigh & Bryant 2015) with default settings.

231

### 232 *Demographic reconstruction*

233 We used the codon-partitioned concatenated protein-coding regions of the sperm whale  
234 mitogenomes (excluding *NADH6* following Alexander *et al.* 2013; Ho & Lanfear 2010)  
235 in a skygrid analysis (implemented in BEAST v1.8.3; Drummond *et al.* 2012) and a  
236 skyline analysis (implemented in BEAST v2.3.0; Bouckaert *et al.* 2014). All 175 samples  
237 were included in both analyses to approximate a “balanced” sampling strategy (multiple  
238 samples from multiple populations) found to result in the least bias in inferring  
239 demographic change (Heller *et al.* 2013), and a separate GTR+G+I substitution model  
240 was used for each codon partition. Prior shapes for parameters within the substitution  
241 models and the relative rates for each codon position were derived from Alexander *et al.*  
242 (2013) (summarized in supplemental Table S2). For the skygrid analysis, two chains of  
243 100M states, sampling every 100,000 states, were run. For the skyline analysis, two  
244 chains of 50 million states with sampling every 10,000 states were carried out.  
245 Convergence was assessed for the two analyses by comparing posterior distributions  
246 between chains in TRACER v1.6, and for topologies through RWTY. Demographic

247 reconstructions were generated through TRACER. Model comparison was performed in  
248 TRACER using AICM with 1,000 bootstraps (Baele *et al.* 2012).

249

250 For demographic analysis based on the nuclear genome, we employed pairwise  
251 sequentially Markovian coalescent (PSMC; Li & Durbin 2011) analysis of three sperm  
252 whale high-coverage genomes to infer changes in effective population size ( $N_e$ ). We  
253 aligned published short read data from three sperm whales (GMX-SRS38925; BioSample  
254 SAMN01906698 (reference genome, Gulf of Mexico); read files SRR680161,  
255 SRR680169, SRR674482; SC991024-177-1; BioSample SAMN06187412 (Pacific); read  
256 files SRR5136496, SRR5136506, SRR5136508, SRR5146847; BioSample  
257 SAMN06187413 (Indian); read files SRR5136491, SRR5136493, SRR5136497,  
258 SRR5146843), to the repeat-masked sperm whale reference genome v2.0.2 (accession  
259 No. GCA\_000472045.1; Warren *et al.* 2017b). Details of read quality filtering and  
260 assembly are provided with supplemental Figure S1. The PSMC plot was scaled to an  
261 autosomal mutation rate ( $\mu_A$ ) of  $2.9 \times 10^{-8}$  substitutions per nucleotide per generation  
262 (Dornburg *et al.* 2012) and a generation time of 31.9 years (Taylor *et al.* 2007), and we  
263 conducted 100 bootstrap resamplings on all PSMC analyses. Sensitivity testing for  
264 different mutation rates and generation times were conducted by re-scaling the PSMC  
265 plots (see supplemental Figure S1). While PSMC can provide useful insights into  
266 demographic change inferred from changes in coalescent rates (Li & Durbin 2011), it is  
267 also sensitive to changes in population structure (Mazet *et al.* 2016). Therefore, we  
268 extended the PSMC analyses presented by Warren *et al.* (2017b) by also carrying out  
269 PSMC analysis of a pseudo-diploid genome made by randomly sampling an allele at each  
270 site from each of the individual genome assemblies using seqtk  
271 (<https://github.com/lh3/seqtk>; see supplemental Figure S1 for details). The pseudo-  
272 diploid analysis provides information on changes in the rate of coalescence between two  
273 individual genomes through time, and therefore the timing of changes in population  
274 structure relative to the changes in  $N_e$  inferred by the single genome PSMC analyses (see  
275 Cahill *et al.* 2016; Chikhi *et al.* 2018).

276

277 *Ancestral range reconstruction*

278 For biogeographic ancestral range reconstruction analyses, the full mitogenome  
279 phylogeny was pruned to twelve clades that had high posterior support. A custom R-  
280 script was then used to prune the tree topology to one branch per clade (N. Matzke;  
281 [http://phylo.wikidot.com/example-biogeobears-scripts#pruning\\_a\\_tree](http://phylo.wikidot.com/example-biogeobears-scripts#pruning_a_tree)). The terminal  
282 branches were assigned to ocean basin(s) based on the origins of samples found within  
283 the non-pruned clades, and the tree and geographic information were used for  
284 biogeographic analysis using the R package BioGeoBEARS (Matzke 2012, 2013). The  
285 package was used to compare three basic models (DEC, DIVALIKE, BAYARELIKE),  
286 and two forms of each model (with and without founder-event cladogenesis; Matzke  
287 2014). These models allowed for different combinations of range expansion, range  
288 splitting (vicariance), and extinction, with the model conferring the highest likelihood on  
289 the tip data selected based on AIC. Likelihood ratio tests were used to compare the nested  
290 models, with and without founder-event cladogenesis. Clades were subsampled to test for  
291 the effect of uneven sampling (see methods in the legend of supplemental Figure S2).

292

293 Suitable-habitat maps were generated with the AquaMaps approach to species  
294 distribution modelling (Kaschner *et al.* 2016; Kaschner *et al.* 2011; Ready *et al.* 2010)  
295 based on physical and oceanographic parameters for the last glacial maximum (LGM,  
296 ~20 KYA), current, and future conditions (year 2100, based on IPCC A2 emissions  
297 scenario). Since adult male and female sperm whales have different habitat use patterns,  
298 with males migrating to higher latitudes to feed, we altered the global sperm whale  
299 suitable habitat model (males and females) to generate female-specific models by setting  
300 the minimum mean sea surface temperature (minSST, preferred minSST) to approximate  
301 the observed summer distributions of adult female and mixed family groups in the North  
302 Pacific identified from commercial whaling records (Ivashchenko *et al.* 2014). The  
303 adjusted mean SST does not perfectly reflect the summer SST patterns, but allows  
304 approximate habitat models for the different time periods. All models exclude the  
305 primary production envelope because this information is not available for the LGM, but  
306 comparison of the present-day distribution maps with and without primary production  
307 indicated little effect of this parameter (supplemental Figure S3 A-D,  
308 [www.aquamaps.org](http://www.aquamaps.org), supported by previous research that suggested little correlation of

309 primary production with sperm whale distributional patterns: Jaquet & Whitehead 1996).  
310 Total sizes of distributions were subsequently calculated for both sexes in different ocean  
311 basins for all three time periods. We calculated areas using both a probability threshold of  
312 0.0 (approximating the mean annual native range of a species including some potentially  
313 lesser utilized habitat) and  $\geq 0.6$  (shown to correspond to the core habitat of a species;  
314 Kaschner *et al.* 2011).

315

#### 316 *Selection analyses on mitogenome data*

317 We aligned the codon-partitioned concatenated protein coding regions of newly  
318 generated sperm whale mitogenomes with the multispecies mitogenome alignment of  
319 Alexander *et al.* (2013), and updated this with more recently published cetacean  
320 mitogenomes/refseq versions of cetacean mitogenomes (see supplemental Table S3 for  
321 all accession numbers). Using the priors detailed in supplemental Table S4, and a Yule  
322 model of speciation, we ran two chains of 100 M generations sampling every 1,000 states  
323 in BEAST v2.3.0. After checking for convergence using TRACER and AWTY (Nylander  
324 *et al.* 2008; Wilgenbusch *et al.* 2004), we used the tree we obtained for tree-based  
325 analyses of selection using TreeSAAP v3.2 (Woolley *et al.* 2003) and PAML v4.9 (Yang  
326 2007). In addition to these methods, we estimated selection for each codon using HyPhy  
327 (Pond *et al.* 2005) as implemented in MEGA v6.06 (Tamura *et al.* 2013). We further  
328 examined selection using the MEME (Murrell *et al.* 2012) and FUBAR methods (Murrell  
329 *et al.* 2013), as implemented on the Datamonkey webserver (Delpont *et al.* 2010; Pond &  
330 Frost 2005). MEME is designed to detect sites that have experienced episodic  
331 diversification, while FUBAR is designed to detect sites that have experienced pervasive  
332 diversification. We used both methods to detect any sites that have experienced positive  
333 selection in the sperm whale. We conducted all of these analyses using just one  
334 representative sperm whale haplotype (mtGen01), and GTR models of nucleotide  
335 substitution (or REV models where GTR was not available). For investigating specific  
336 sites inferred to be under positive selection we used  $\alpha = 0.05$  as the threshold for  
337 statistical significance in HyPhy, MEME and FUBAR. Within PAML M8, we used  
338 Bayes Empirical Bayes (BEB) (Yang *et al.* 2005), with a threshold of  $P > 95\%$ .  
339 TreeSAAP results were restricted to putative sites under selection where at least one

340 property had a magnitude category of six or more in every pairwise comparison between  
341 the representative sperm whale and other cetaceans.

342

343 Following Caballero et al. (2015), 3D homology models of proteins for genes where  
344 positive selection was detected in sperm whales (*ND1*, *ND2*, *ATP8*, *COX3*, *ND4L*, *COX3*,  
345 *ND4*, *ND5*, *CYTB*) were generated by the SWISS-MODEL server (Schwede *et al.* 2003),  
346 using the templates specified in supplemental Figure S4 (best-fitting model based out of  
347 the top four templates for each gene region), and visualized using UCSF Chimera v1.11  
348 (Pettersen *et al.* 2004). This 3D model was annotated with domains based on alignment to  
349 the best-fitting template. We annotated a 2D model constructed with Protter (Omasits *et*  
350 *al.* 2014) with the domains and transmembrane topology based on alignment with the  
351 template, as well as additional secondary structure from the 3D model of the sperm whale  
352 constructed using DPSS (Kabsch & Sander 1983).

353

## 354 **Results**

### 355 *Mitogenome dataset assembly*

356 We generated mitogenome sequences for 158 new samples for this study. After  
357 combining these with 17 previously published sequences from Alexander et al. (2013),  
358 our dataset consisted of 175 globally distributed mitogenomes (Figure 1). We replicated  
359 three sequences from Alexander et al. (2013) using our capture enrichment methods and  
360 verified consistency between our approach and the long-range PCR approach of  
361 Alexander et al. (2013). Mean depth of coverage was 126× (range 18-170), and all but 13  
362 of the newly generated sequences contained  $\leq 10$  unresolved or missing nucleotides  
363 (maximum = 65). After alignment and verification of unique indels and variant sites,  
364 there were 80 unique haplotype sequences (Table S5).

365

### 366 *Genetic diversity analyses and relationship of haplotypes*

367 Mitogenome nucleotide diversity ( $\pi = 0.093\%$ ) was very similar to that reported  
368 previously for samples predominantly obtained near New Zealand (0.096%, Alexander *et*  
369 *al.* 2013) despite a 10-fold increase in sample size and global sample distribution. This  
370 estimate may still be slightly inflated due to selection of some specimens to maximize

371 coverage of control region haplotype diversity both in this study and in Alexander *et al.*  
372 (2013). Sperm whales have some of the lowest documented mitogenomic diversity  
373 among cetaceans (see Table 1 in Alexander *et al.* 2013), but haplotype diversity was high  
374 overall (0.975) and differed significantly by ocean basin in all comparisons except “main  
375 basin” Atlantic vs. Gulf of Mexico (GoMx: both haplotype and nucleotide diversity) and  
376 Pacific vs. GoMx (nucleotide diversity) (Table 1; supplemental Table S6). Differences in  
377 diversity remained significant for all comparisons except GoMx vs. Mediterranean  
378 (haplotype diversity) even after removal of replicate haplotypes collected from the same  
379 social group to control for oversampling of close relatives (supplemental Table S6).

380

### 381 *Phylogenetic analyses*

382 The time calibrated phylogeny for TMRCA of the four divergent sperm whale haplotypes  
383 with outgroups (Phase I) is in supplemental Figure S5. The mean substitution rate  
384 estimate for all codons was 7.596E-3 substitutions/site/Myr (95% CI = 6.357E-3 –  
385 8.860E-3), lower than that estimated previously for the sperm whale (1.04E-2) and  
386 odontocetes (1.0E-2) based on different parameters (Alexander *et al.* 2013). The median  
387 TMRCA estimate of 136.7 KYA (95% CI = 85.1 – 201.1 KYA) was used as the prior for  
388 analysis of the full set of sperm whale haplotypes (Phase II). The input xml, log and  
389 output trees files are available in the Dryad digital archive (doi:10.5061/dryad.57271).

390 The sperm whale phylogeny based on the full set of complete mitogenome haplotypes is  
391 shown in Figure 2. All equivalent sample size (ESS) values were >200 and RWTY  
392 indicated convergence of topology among separate runs. The median TMRCA estimates  
393 from the full-length mitogenomes and the 3<sup>rd</sup> positions of concatenated coding loci were  
394 nearly identical: 126.4 KYA (95% CI = 81.04 – 180.8 KYA) and 126.5 KYA (80.066 -  
395 178.4), respectively. These estimates were older than the TMRCA estimated based on 17  
396 mitogenomes from the Pacific alone (103 KYA (95% HPD 72.8 - 137.4); Alexander *et al.*  
397 *al.* 2013), likely due to the lower median substitution rate inferred in the current analysis  
398 (7.034E-3 substitutions per site per million years: 95% CI = 4.068E-3 – 1.078E-2). The  
399 input xml, log and output trees files are available in the Dryad digital archive  
400 (doi:10.5061/dryad.57271).

401

402 Full length mitogenome haplotypes tended to be separated by only a few nucleotide  
403 substitutions (Figure 3). Despite this low diversity, a high degree of phylogeographic  
404 structure was evident: 65 of the 80 haplotypes were found only in the Pacific, 14 were  
405 found only in the Atlantic, and only one haplotype (mt03) was found in both of these  
406 ocean basins (1x N. Pacific, 9x N. Atlantic). Sampling in the Indian Ocean was limited to  
407 one sample from the Maldives that had a unique haplotype (mt33) that differed by 1 bp  
408 from a haplotype found in Tasmania (mt04). One additional Indian Ocean mitogenome  
409 (from the Seychelles) assembled from the genome data of Warren et al. (2017b) was  
410 haplotyped as mt54, also found in the Tasmania. The three most common control region  
411 (CR) haplotypes globally (A, B, C based on 394bp; supplemental Table S7; Alexander *et*  
412 *al.* 2016), which are shared between the Pacific and Atlantic Oceans (and the  
413 Mediterranean Sea), constituted 67% of the samples used in this study. These three CR  
414 haplotypes were further divided into 17, 16, and 14 mitogenome haplotypes, respectively,  
415 and the four samples from the Mediterranean Sea, all CR haplotype C, were split into two  
416 unique haplotypes (supplemental Table S7). Apart from mt03 (CR haplotype A),  
417 mentioned above, all of the 48 mitogenome haplotypes corresponding to these three CR  
418 haplotypes were ocean-basin specific.

419

420 We conducted random forest analysis to determine the probability of assigning known  
421 and newly discovered mitogenome haplotypes to ocean basin. When the GoMx and  
422 Mediterranean (Med.) samples were collapsed into the Atlantic population for purposes  
423 of assignment, results indicated 100% probability of correct assignment to the Pacific, but  
424 only 78% probability for the Atlantic Ocean (Table 2). Without the GoMx and Med.  
425 samples, the assignment probability was slightly lower for the Atlantic (71%). The large  
426 number of ocean-specific haplotypes (all but one shared Pacific/Atlantic haplotype) could  
427 suggest high diagnosability, but the lower success is due to both the single shared  
428 haplotype (mt03) and high similarity of several Atlantic haplotypes to Pacific haplotypes  
429 (Figures 2, 3).

430

431 *Demographic reconstruction*

432 The two skygrid chains showed convergence, and all skygrid parameters had ESS values  
433 above 200. The estimated TMRCA was 87 KYA (95% HPD: 60.3-119.4). The skyline  
434 analysis also showed convergence between both chains, and all parameters had ESS  
435 values >200 after combining the chains. A TMRCA very similar to the skygrid analysis  
436 was recovered (Median: 86 KYA; 95% HPD: 59-118.8 KYA). The optimal model based  
437 on AICM was the skyline. Both analyses showed patterns consistent with a population  
438 expansion (Figure 4), but the timing appeared to differ, with the skyline suggesting the  
439 expansion began 30-35 KYA and the skygrid analysis suggesting a more gradual increase  
440 from >80 KYA (Figure 4). The 95% confidence intervals for the two methods indicate  
441 little resolution in the timing of the population expansion. Since these analyses used all  
442 samples from both ocean basin populations, assumptions of the models were violated.  
443 However, when limiting the sample set to only the Atlantic or Pacific Oceans  
444 (supplemental Figure S6), the pattern of population expansion is still recovered for the  
445 Pacific, the location of the inferred mitogenome MRCA (see ancestral reconstruction  
446 section). In contrast, the skyline plot is flat for the Atlantic, as might be expected where  
447 mitogenome clusters do not coalesce within the ocean basin. Input xml and output log  
448 and tree files are available in the Dryad digital archive (doi:10.5061/dryad.57271).

449

450 Although the nuclear genome PSMC analysis also recovered evidence of a recent  
451 population expansion, it indicated that this expansion was just one in a series of  
452 population fluctuations through time. Plots from analysis of all three ocean-basin samples  
453 declined starting about 2-3 million years ago (MYA) to a low around 1 MYA, with some  
454 fluctuation through the early and mid-Pleistocene climate cycles (Figure 4). In the late  
455 Pleistocene, the low effective population size ( $N_e$ ) approximately 120 -150 KYA, appears  
456 to have increased to a peak  $N_e$  roughly 50 KYA, then declined again to a low at about 20-  
457 30 KYA just before the last glacial maximum (Figure 4). This pattern is nearly identical  
458 between samples from the Atlantic, Pacific and Indian Oceans, differing only during the  
459 last glacial cycle, where the estimated population size estimate in the Atlantic was lower  
460 (though variation is higher, so differences are less certain; Supplemental Figure S1).  
461 These results are concordant with previous PSMC analyses of sperm whales (Warren *et*  
462 *al.* 2017b). However, the y-axis of a PSMC plot is most accurately interpreted as the

463 inverse of the coalescent rate, and changes in population structure can wrongly be  
464 interpreted as changes in effective population size using this method (Foote *et al.* 2016;  
465 Mazet *et al.* 2015; Mazet *et al.* 2016). To further tease apart changes in structure from  
466 changes in effective population size, we generated pseudo-hybrids of pairs of individuals  
467 from different populations (Cahill *et al.* 2016). As populations undergo a gradual fission,  
468 the rate coalescence between the two haploid genomes that comprise the pseudo diploid  
469 will decline forward in time, and should cease altogether when the two populations are  
470 completely isolated (Cahill *et al.* 2016). PSMC will thus infer a gradual increase in  $N_e$  as  
471 the coalescence rate decreases, and an infinite increase in effective population size at the  
472 point in time when the lineages become completely isolated.

473  
474 PSMC analyses of the pseudo-diploids indicate high uncertainty at >1 MYA, but closely  
475 resemble the shared  $N_e$  of the three ocean-specific samples 0.15-1 MYA, indicative of a  
476 stable rate of coalescence between lineages (although possibly still structured, see Chikhi  
477 *et al.* 2018) during this period (Figure 4). During the Eemian inter-glacial, at around 120  
478 KYA, the pseudo-diploid estimates of  $N_e$  increase rapidly and abruptly rises to infinity  
479 for all three population-pair pseudo-diploids. We interpret this as indicative of divergence  
480 between sperm whale populations associated with colonization of ocean-basins at this  
481 time. Immediately following this period, estimates of  $N_e$  fall in both the Atlantic and  
482 Pacific (and to a lesser extent, the Indian Ocean) individual PSMC plots. We interpret  
483 these combined inferences as being indicative that the population split started in the  
484 Eemian, likely with some ongoing gene flow (resulting in additional coalescence events  
485 leading to the PSMC inferring a larger  $N_e$  in all samples), and that gene flow (and hence  
486 coalescence) then ceased altogether after the Eemian, leading to the inferred decline in  $N_e$   
487 by PSMC in the individual samples. Thus, the increase and then decline in inferred  $N_e$  for  
488 each ocean between ~125,000 and 20,000 years ago is likely to be an artifact of  
489 population differentiation, masking the true effective population sizes.

490

491 *Ancestral range reconstruction and suitable habitat models*

492 Biogeographic ancestral range reconstruction analyses with BioGeoBEARS found  
493 dispersal-extinction-cladogenesis (DEC) as the most likely model, with the nested form

494 of the model allowing for founder-event cladogenesis (DEC+J) significantly more likely  
495 than the traditional DEC model ( $p = 0.0057$ ). The resulting phylogeographic inference for  
496 the pruned tree indicates that the root of the tree was in the Pacific, with multiple  
497 colonizations of the Atlantic around approximately 20,000 and 60,000 years ago (Figure  
498 5). The majority of our samples originated from the Pacific, which could potentially bias  
499 our ancestral area reconstruction (Moyle *et al.* 2016). We examined the effect of this  
500 discrepancy in sample size by down-sampling the Pacific to equal that of the Atlantic (see  
501 supplemental Figure S2). Across  $n = 1,000$  replicates down-sampling the Pacific to 35  
502 individuals, the root of the tree was inferred as Pacific in 99.9% of the replicates,  
503 indicating that uneven sampling is not driving this pattern.

504

505 Suitable habitat models for females in particular show a striking change between the  
506 present-day and the LGM, especially in the Atlantic Ocean (Figure 6), where core  
507 suitable habitat for females was reduced by 50% at the LGM (supplemental Table S8).  
508 The latitudinal shift also indicates that the Atlantic and Pacific habitats were likely  
509 completely separated by land masses, with only marginal potential for female dispersal  
510 between ocean basins even in the current warmer period. Projections of future habitat at  
511 the beginning of the next century suggest that dispersal between ocean basins may be  
512 more likely, but that northern and southern hemisphere populations may become  
513 separated (supplemental Figure S3).

514

#### 515 *Selection analyses on mitogenome data*

516 PAML detected a pervasive pattern of purifying selection across the cetacean  
517 mitogenomes (supplemental Table S9), with the ratio of non-synonymous to synonymous  
518 changes estimated as  $\omega = 0.093$ . However, all methods except FUBAR detected at least  
519 one site putatively under positive selection in the lineage leading to sperm whales (after  
520 restricting sites inferred to be under positive selection to those where all sperm whales  
521 showed a fixed amino acid substitution in comparison with the rest of the cetacean  
522 species, supplemental Table S10). In total, 19 amino acids spanning 8 mitochondrial-  
523 encoded proteins were found to show signatures of positive selection in the sperm whale  
524 (supplemental Table S10, Figure S4). Of these 19 amino acid changes, 12 of them

525 occurred in or adjacent to transmembrane regions, contrasting with the overall pattern of  
526 mammalian evolution of most adaptive variation being restricted to loop regions (da  
527 Fonseca *et al.* 2008).

528

## 529 **Discussion**

530 Despite the high abundance and global extent of the sperm whale's distribution,  
531 mitogenomic diversity within this species is markedly low (this study; Alexander *et al.*  
532 2013; Lyrholm & Gyllensten 1998; Whitehead 2005). However, without detailed  
533 examination of demographic patterns indicated by the nuclear genome, previous research  
534 was unable to distinguish between demographic causes and selective sweeps as the most  
535 likely cause of this low diversity. Here, we showed that both the mitogenome and nuclear  
536 genome analyses provide evidence of a population expansion and ocean-basin divergence  
537 since the last interglacial period. The presence of this pattern across both genomes is  
538 consistent with a historically small effective population size (suggested by the PSMC  
539 plots for all three ocean basins) rather than selective sweeps on the mitogenome or  
540 cultural hitchhiking of haplotypes as the primary cause of low mtDNA diversity in sperm  
541 whales, despite our detection of sites under positive selection in the sperm whale  
542 mitogenome. In contrast, the expectation proposed under the mitochondrial selective  
543 sweep hypotheses (due to either direct selection on the mitogenome or a matrilineal  
544 cultural trait, and hitchhiking of linked neutral mtDNA diversity) is discordant patterns  
545 between the nuclear and mitochondrial genomes, with a decline in mitochondrial  
546 diversity over time (Whitehead 2005) but limited or no concomitant decline in nuclear  
547 DNA diversity. This expectation is at least partially due to the high rates of sex-specific  
548 dispersal of males in sperm whales (Alexander *et al.* 2016), and recombination in the  
549 nuclear genome, unlinking the nuclear and mitochondrial genomes in these processes.  
550 However, it is important to note that given the strong influence of social structure on  
551 sperm whales (Whitehead *et al.* 2017), and the detection of positive selection on the  
552 protein-coding regions, we cannot rule out other forces, including cultural hitchhiking,  
553 having further reduced mitogenome diversity in the sperm whale. Nevertheless, the  
554 consistency of the inferred reduction in population size based on the nuclear genome  
555 occurring at approximately the same time as the TMRCA of the mitogenomes suggests

556 demographic processes as the primary cause of low present-day sperm whale mtDNA  
557 diversity.  
558  
559 Our mitogenomic analyses suggest that the current global distribution of sperm whales  
560 results from a relatively recent expansion (20-40 KYA). The inferred mitogenomic  
561 MRCA suggests expansion from a single, refugial population most likely located in the  
562 Pacific Ocean (though we cannot rule out an Indian Ocean refugium due to lack of  
563 sampling). “Ice-house” conditions are believed to have developed approximately 3 MYA,  
564 characterized by the development of perennial Arctic Ocean sea ice and continental ice  
565 sheets in North America and Eurasia (Greene *et al.* 2008). This global change has been  
566 implicated in a global extinction event among marine megafauna (Pimiento *et al.* 2017)  
567 and coincides with an inferred decline in the global sperm whale population (revealed by  
568 PSMC analyses of individual sperm whale genomes), and an evident restriction in the  
569 distribution of sperm whales (revealed by pseudo-diploid PSMC analysis of the nuclear  
570 genome, Figure 4), potentially reducing the distribution to a single refugial population  
571 from which present day sperm whale lineages descended. The global abundance appears  
572 to have increased from a low of <10,000 breeding individuals ( $N_e$ ) since the last long  
573 cold period (Saale glaciation, ~80 kyr) that ended approximately 125 KYA. Since then,  
574 there have been several shorter cold periods, lasting <10 kyr each (Figure 4), which  
575 appear to correspond approximately with coalescence nodes in the mitogenome tree  
576 (Figure 2), after which haplotypes diversified and mitochondrial lineages dispersed  
577 between oceans. Although timing estimates are approximate, the pattern suggests effects  
578 of climate on population size, distribution, and persistence of specific maternal lineages  
579 through time in the sperm whale. While male sperm whales are known to travel to and  
580 feed in cold temperate/polar waters, females are generally restricted to warmer tropical  
581 and temperate waters, and mtDNA data suggest that they may only be able to disperse  
582 between the Pacific and Atlantic oceans during warm periods that allow them to extend  
583 their latitudinal range. However, the pseudo-diploid analysis and divergence of the  
584 nuclear genome PSMC plots from samples located in different oceans over the last  
585 ~100,000 years (Figure 4) both suggest that males also rarely disperse between ocean  
586 basins, resulting in genetic divergence between the Atlantic and Pacific (see also

587 Alexander *et al.* 2016; Lyrholm & Gyllensten 1998; Lyrholm *et al.* 1999). Nuclear  
588 genome-wide SNP analysis of more samples from each ocean basin – particularly the  
589 under-sampled Indian Ocean – will be needed to infer degree of divergence and levels of  
590 current and/or historical gene flow.

591

592 The use of complete mitogenomes instead of control region sequences allows for  
593 substantially greater power to detect phylogeographic structure in low-diversity species  
594 such as the sperm whale, and can also improve power in population genetic studies. The  
595 sampling design for this study was not appropriate for traditional frequency-based  
596 population genetic analyses, but comparative analysis of mitogenome and control region  
597 haplotypes for large geographic regions (supplemental Figure S7) indicated mitogenomes  
598 were more sensitive at detecting significant differentiation among strata based on  $F_{ST}$ ,  
599  $\Phi_{ST}$  and  $\chi^2$  statistics. Although patterns of differentiation were largely concordant  
600 between these data sets, the lack of power from control region data indicates caution must  
601 be used when genetic structure among potential strata is not detected solely based on CR  
602 data.

603

604 Sperm whales are among the deepest diving marine mammals, and it is likely that their  
605 mitochondrially-encoded proteins have been under intense selection for oxygen  
606 efficiency (Janik 2001) and robustness to pressure changes (Somero 1992; Warren *et al.*  
607 2017b). Changes in transmembrane regions could more strongly affect protein structure  
608 and function than in the loop regions (Saier 1994), potentially directly addressing these  
609 selective pressures. Future comparisons to patterns of positive selection on other deep-  
610 diving species would be needed to see if this was a pervasive pattern across other taxa

611

612 Sperm whales are not considered rare, but have been depleted to approximately 1/3 of  
613 their pre-whaling population sizes and are protected by various national and international  
614 laws and treaties (e.g., the US Endangered Species Act, IUCN Red List, International  
615 Whaling Commission). Given evidence of population structure within and between ocean  
616 basins (Alexander *et al.* 2016; Engelhaupt *et al.* 2009; Lyrholm & Gyllensten 1998;  
617 Mesnick *et al.* 2011), the likelihood that populations were unevenly depleted by whaling

618 (Ivashchenko *et al.* 2014), and lack of information on population recovery globally, it is  
619 highly probable that some sperm whale populations are still endangered or at risk (Carroll  
620 *et al.* 2014; Gero & Whitehead 2016; Notarbartolo-Di-Sciara 2014). Our results provide  
621 support for current isolation of populations located in different ocean basins, with  
622 episodic dispersal of females restricted to only warm climate periods. Although the  
623 current warming trends predict expansion of sperm whale habitat that allows both growth  
624 and opportunities for inter-ocean dispersal, we cannot predict how rapid climate change  
625 may affect the ecosystems on which sperm whales depend (see, e.g., Dawe *et al.* 2007;  
626 Ibanez *et al.* 2011; Jaquet *et al.* 2003; Pecl & Jackson 2008). In particular, climate change  
627 can affect the Atlantic and Pacific oceans quite differently (Boyle & Keigwin 1985;  
628 Cheng *et al.* 2009; Greene *et al.* 2008; Howard 1997), which may explain the apparent  
629 refugial population of sperm whales in the Pacific Ocean during the last long glacial  
630 period. Further research on trends in abundance and health of sperm whale populations  
631 and protection from other anthropogenic effects such as pollution (e.g., de Stephanis *et*  
632 *al.* 2013; Savery *et al.* 2014a; Savery *et al.* 2014b; Unger *et al.* 2016), ocean noise (Mate  
633 *et al.* 1994), ship strikes (Jensen & Silber 2003), entanglement (Barlow & Cameron  
634 2003), and prey competition (Hucke-Gaete *et al.* 2004) should be top priorities to prevent  
635 loss of already depleted populations.

636

637

### 638 **Acknowledgements**

639 We are grateful to all who collected and contributed samples used in this study: Marie  
640 Hill of the PIFSC Cetacean Research Program and Joint Institute for Marine and  
641 Atmospheric Research, Erin Oleson (PIFSC), Allan Ligon, Adam Ü, Mark Deakos, the  
642 Commander, U.S. Pacific Fleet, Office of Naval Research and Living Marine Resources  
643 Programs, Diane Claridge, John Durban, Kim Parsons, Luke Rendell, Barb Taylor,  
644 Louella Dolar, William Perrin, Deborah Thiele, Karen Evans, Robert Pitman, Tim  
645 Gerrodette, Tom Jefferson, Samuel Hung, Liz Slooten, Sophie Laran, Emilie Praca, Lisa  
646 Ballance, Paul Wade, William McLellan, Ken Balcomb, Aleta Hohn, Jay Barlow, Dan  
647 Odell, Hisao Azuma, Christine Adkins, Wayne Haggard, Lars Kleivane, Manuel Furtado  
648 Neto, Sue Barco, Wayne McFee, K. Mullin, and the Southeast US marine mammal

649 stranding network. All samples have been imported to the US under CITES permit, and  
650 samples from the US were collected under Marine Mammal Protection Act permits. We  
651 are grateful for technical and analytical assistance from The Scripps Research Institute  
652 core sequencing lab, Sebastian Duchene, Simon Ho, D. Steel, K. Hoekzema, C. Sislak  
653 and Milaya Nykänen. Cristina Garilao generously provided customized distribution maps  
654 from AquaMaps. We are very grateful for helpful discussion and comments on the  
655 manuscript provided by Hal Whitehead, Kim Parsons, Karen Chambers and four  
656 anonymous reviewers. Funding was provided by the National Marine Fisheries Service  
657 Southwest Region; the Marine Mammal and Turtle Division, Southwest Fisheries  
658 Science Center; U.S. Navy Pacific Fleet and NMFS Pacific Islands Science Center.  
659 Financial support for ADF was provided by the Welsh Government and Higher  
660 Education Funding Council for Wales through the Sêr Cymru National Research  
661 Network for Low Carbon, Energy and Environment, and from the European Union's  
662 Horizon 2020 research and innovation programme under the Marie Skłodowska-Curie  
663 grant agreement No 663830.

664

665

666

## 667 **References**

- 668 Alexander A, Steel D, Hoekzema K, Mesnick SL, Engelhaupt D, Kerr I, . . . Baker CS  
669 (2016) What influences the worldwide genetic structure of sperm whales  
670 (*Physeter macrocephalus*)? *Molecular Ecology* **25**, 2754-2772.
- 671 Alexander A, Steel D, Slikas B, Hoekzema K, Carraher C, Parks M, . . . Baker CS (2013)  
672 Low diversity in the mitogenome of sperm whales revealed by next-generation  
673 sequencing. *Genome Biology and Evolution* **5**, 113-129.
- 674 Amos W (1999) Culture and genetic evolution in whales. *Science* **284**, 2055a.
- 675 Archer FI, Adams PE, Schneiders BB (2017a) strataG: An R package for manipulating,  
676 summarizing, and analyzing population genetic data. *Molecular Ecology*  
677 *Resources* **17**, 5-11.
- 678 Archer FI, Martien KK, Taylor BL (2017b) Diagnosability of mtDNA with Random  
679 Forests: Using sequence data to delimit subspecies. *Marine Mammal Science* **33**,  
680 101-131.
- 681 Archer FI, Morin PA, Hancock-Hanser BL, Robertson KM, Leslie MS, Berube M, . . .  
682 Taylor BL (2013) Mitogenomic phylogenetics of fin whales (*Balaenoptera*  
683 *physalus* spp.): genetic evidence for revision of subspecies. *PLoS ONE* **8**, e63396.
- 684 Baele G, Lemey P, Bedford T, Rambaut A, Suchard MA, Alekseyenko AV (2012)  
685 Improving the accuracy of demographic and molecular clock model comparison

- 686 while accommodating phylogenetic uncertainty. *Molecular Biology and Evolution*  
 687 **29**, 2157-2167.
- 688 Baker CS, Slade RW, Bannister JL, Abernethy RB, Weinrich MT, Lien J, . . . Palumbi  
 689 SR (1994) Hierarchical structure of mitochondrial DNA gene flow among  
 690 humpback whales *Megaptera novaeangliae*, world-wide. *Molecular Ecology* **3**,  
 691 313-327.
- 692 Baker CS, Steel D, Calambokidis J, Falcone E, Gonzalez-Peral U, Barlow J, . . .  
 693 Yamaguchi M (2013) Strong maternal fidelity and natal philopatry shape genetic  
 694 structure in North Pacific humpback whales. *Marine Ecology Progress Series*  
 695 **494**, 291-306.
- 696 Bandelt H-J, Forster P, Röhl A (1999) Median-joining networks for inferring  
 697 intraspecific phylogenies. *Molecular Biology and Evolution* **16**, 37-48.
- 698 Barlow J, Cameron GA (2003) Field experiments show that acoustic pingers reduce  
 699 marine mammal bycatch in the California drift gill net fishery. *Marine Mammal*  
 700 *Science* **19**, 265-283.
- 701 Bazin E, Glemin S, Galtier N (2006) Population size does not influence mitochondrial  
 702 genetic diversity in animals. *Science* **312**, 570-572.
- 703 Bouckaert R, Heled J, Kuhnert D, Vaughan T, Wu CH, Xie D, . . . Drummond AJ (2014)  
 704 BEAST 2: a software platform for Bayesian evolutionary analysis. *PLoS Comput*  
 705 *Biol* **10**, e1003537.
- 706 Boyle EA, Keigwin LD (1985) Comparison of Atlantic and Pacific paleochemical  
 707 records for the last 215,000 years - changes in deep ocean circulation and  
 708 chemical inventories. *Earth and Planetary Science Letters* **76**, 135-150.
- 709 Breiman L (2001) Random forests. *Machine Learning* **45**, 5-32.
- 710 Buddhakosai W, Klinawat W, Smith O, Sukmak M, Kaolim N, Duangchantrasiri S, . . .  
 711 Wajjwalku W (2016) Mitogenome analysis reveals a complex phylogeographic  
 712 relationship within the wild tiger population of Thailand. *Endangered Species*  
 713 *Research* **30**, 125-131.
- 714 Caballero S, Duchene S, Garavito MF, Slikas B, Baker CS (2015) Initial evidence for  
 715 adaptive selection on the NADH subunit two of freshwater dolphins by analyses  
 716 of mitochondrial genomes. *PLoS ONE* **10**, e0123543.
- 717 Cahill JA, Soares AE, Green RE, Shapiro B (2016) Inferring species divergence times  
 718 using pairwise sequential Markovian coalescent modelling and low-coverage  
 719 genomic data. *Philosophical Transactions of the Royal Society of London B,*  
 720 *Biological Sciences* **371**.
- 721 Carroll G, Hedley S, Bannister J, Ensor P, Harcourt R (2014) No evidence for recovery in  
 722 the population of sperm whale bulls off Western Australia, 30 years post-whaling.  
 723 *Endangered Species Research* **24**, 33-43.
- 724 Cheng H, Edwards RL, Broecker WS, Denton GH, Kong XG, Wang YJ, . . . Wang XF  
 725 (2009) Ice age terminations. *Science* **326**, 248-252.
- 726 Chikhi L, Rodriguez W, Grusea S, Santos P, Boitard S, Mazet O (2018) The IICR  
 727 (inverse instantaneous coalescence rate) as a summary of genomic diversity:  
 728 insights into demographic inference and model choice. *Heredity (Edinb)* **120**, 13-  
 729 24.
- 730 da Fonseca RR, Johnson WE, O'Brien SJ, Ramos MJ, Antunes A (2008) The adaptive  
 731 evolution of the mammalian mitochondrial genome. *BMC Genomics* **9**, 119.

- 732 Darriba D, Taboada G, Doallo R, Posada D (2012) jModelTest 2: more models, new  
733 heuristics and parallel computing. *Nature Methods* **9**, 772.
- 734 Dawe EG, Hendrickson LC, Colbourne EB, Drinkwater KF, Showell MA (2007) Ocean  
735 climate effects on the relative abundance of short-finned (*Illex illecebrosus*) and  
736 long-finned (*Loligo pealeii*) squid in the northwest Atlantic Ocean. *Fisheries  
737 Oceanography* **16**, 303-316.
- 738 de Stephanis R, Gimenez J, Carpinelli E, Gutierrez-Exposito C, Canadas A (2013) As  
739 main meal for sperm whales: plastics debris. *Marine Pollution Bulletin* **69**, 206-  
740 214.
- 741 Delport W, Poon AF, Frost SD, Kosakovsky Pond SL (2010) Datamonkey 2010: a suite  
742 of phylogenetic analysis tools for evolutionary biology. *Bioinformatics* **26**, 2455-  
743 2457.
- 744 Dornburg A, Brandley MC, McGowen MR, Near TJ (2012) Relaxed clocks and  
745 inferences of heterogeneous patterns of nucleotide substitution and divergence  
746 time estimates across whales and dolphins (Mammalia: Cetacea). *Molecular  
747 Biology and Evolution* **29**, 721-736.
- 748 Drummond AJ, Suchard MA, Xie D, Rambaut A (2012) Bayesian phylogenetics with  
749 BEAUti and the BEAST 1.7. *Molecular Biology & Evolution* **29**, 1969-1973.
- 750 Engelhaupt D, Hoelzel AR, Nicholson C, Frantzis A, Mesnick S, Gero S, . . . Mignucci-  
751 Giannoni AA (2009) Female philopatry in coastal basins and male dispersion  
752 across the North Atlantic in a highly mobile marine species, the sperm whale  
753 (*Physeter macrocephalus*). *Molecular Ecology* **18**, 4193-4205.
- 754 Finch TM, Zhao N, Korkin D, Frederick KH, Eggert LS (2014) Evidence of positive  
755 selection in mitochondrial complexes I and V of the African elephant. *PLoS ONE*  
756 **9**, e92587.
- 757 Foote AD, Morin PA, Durban JW, Pitman RL, Wade P, Willerslev E, . . . da Fonseca RR  
758 (2011) Positive selection on the killer whale mitogenome. *Biology Letters* **7**, 116-  
759 118.
- 760 Foote AD, Vijay N, Avila-Arcos MC, Baird RW, Durban JW, Fumagalli M, . . . Wolf JB  
761 (2016) Genome-culture coevolution promotes rapid divergence of killer whale  
762 ecotypes. *Nature Communications* **7**, 11693.
- 763 Gero S, Whitehead H (2016) Critical decline of the eastern caribbean sperm whale  
764 population. *PLoS ONE* **11**.
- 765 Greene CH, Pershing AJ, Cronin TM, Ceci N (2008) Arctic climate change and its  
766 impacts on the ecology of the North Atlantic. *Ecology* **89**, S24-38.
- 767 Guindon S, Delsuc F, Dufayard JF, Gascuel O (2009) Estimating maximum likelihood  
768 phylogenies with PhyML. *Methods in Molecular Biology* **537**, 113-137.
- 769 Hancock-Hanser B, Frey A, Leslie M, Dutton PH, Archer EI, Morin PA (2013) Targeted  
770 multiplex next-generation sequencing: Advances in techniques of mitochondrial  
771 and nuclear DNA sequencing for population genomics *Molecular Ecology  
772 Resources* **13**, 254-268.
- 773 Heller R, Chikhi L, Siegismund HR (2013) The confounding effect of population  
774 structure on Bayesian skyline plot inferences of demographic history. *PLoS ONE*  
775 **8**.

- 776 Ho SY, Lanfear R (2010) Improved characterisation of among-lineage rate variation in  
 777 cetacean mitogenomes using codon-partitioned relaxed clocks. *Mitochondrial*  
 778 *DNA* **21**, 138-146.
- 779 Hoelzel AR, Natoli A, Dahlheim ME, Olavarria C, Baird RW, Black NA (2002) Low  
 780 worldwide genetic diversity in the killer whale (*Orcinus orca*): implications for  
 781 demographic history. *Proceedings of the Royal Society B-Biological Sciences*  
 782 **269**, 1467-1473.
- 783 Howard WR (1997) Palaeoclimatology - A warm future in the past. *Nature* **388**, 418-419.
- 784 Huccke-Gaete R, Moreno CA, Arata J, Ctr BW (2004) Operational interactions of sperm  
 785 whales and killer whales with the Patagonian toothfish industrial fishery off  
 786 southern Chile. *Ccamlr Science* **11**, 127-140.
- 787 Ibanez CM, Cubillos LA, Tafur R, Arguelles J, Yamashiro C, Poulin E (2011) Genetic  
 788 diversity and demographic history of *Dosidicus gigas* (Cephalopoda:  
 789 Ommastrephidae) in the Humboldt Current System. *Marine Ecology Progress*  
 790 *Series* **431**, 163-171.
- 791 Ivashchenko YV, Brownell RL, Clapham PJ (2014) Distribution of Soviet catches of  
 792 sperm whales *Physeter macrocephalus* in the North Pacific. *Endangered Species*  
 793 *Research* **25**, 249-263.
- 794 Jackson JA, Steel DJ, Beerli P, Congdon BC, Olavarria C, Leslie MS, . . . Baker CS  
 795 (2014) Global diversity and oceanic divergence of humpback whales (*Megaptera*  
 796 *novaeangliae*). *Proceedings of the Royal Society B-Biological Sciences* **281**.
- 797 Janik VM (2001) Is cetacean social learning unique? *Behavioral and Brain Sciences* **24**,  
 798 337-338.
- 799 Jaquet N, Gendron D, Coakes A (2003) Sperm whales in the Gulf of California:  
 800 Residency, movements, behavior, and the possible influence of variation in food  
 801 supply. *Marine Mammal Science* **19**, 545-562.
- 802 Jaquet N, Whitehead H (1996) Scale-dependent correlation of sperm whale distribution  
 803 with environmental features and productivity in the South Pacific. *Marine*  
 804 *Ecology Progress Series* **135**, 1-9.
- 805 Jensen AS, Silber GK (2003) Large Whale Ship Strike Database, p. 37. National Marine  
 806 Fisheries Service, NOAA Technical Memorandum NMFS-OPR-25, Silver Spring,  
 807 MD.
- 808 Kabsch W, Sander C (1983) Dictionary of protein secondary structure: pattern  
 809 recognition of hydrogen-bonded and geometrical features. *Biopolymers* **22**, 2577-  
 810 2637.
- 811 Kaschner K, Kesner-Reyes K, Garilao C, Rius-Barile J, Rees T, Froese R (2016)  
 812 AquaMaps: Predicted range maps for aquatic species. *World wide web electronic*  
 813 *publication*, [www.aquamaps.org](http://www.aquamaps.org), Version 08/2016.
- 814 Kaschner K, Tittensor DP, Ready J, Gerrodette T, Worm B (2011) Current and future  
 815 patterns of global marine mammal biodiversity. *PLoS ONE* **6**, e19653.
- 816 Kopps AM, Ackermann CY, Sherwin WB, Allen SJ, Bejder L, Krützen M (2014)  
 817 Cultural transmission of tool use combined with habitat specializations leads to  
 818 fine-scale genetic structure in bottlenose dolphins. *Proc Biol Sci* **281**, 20133245.
- 819 Lanfear R, Calcott B, Ho S, Guindon S (2012) PartitionFinder: combined selection of  
 820 partitioning schemes and substitution models for phylogenetic analyses.  
 821 *Molecular Biology and Evolution* **29**, 1695-1710.

- 822 Lang AR, Calambokidis J, Scordino J, Pease VL, Klimek A, Burkanov VN, . . . Taylor  
823 BL (2014) Assessment of genetic structure among eastern North Pacific gray  
824 whales on their feeding grounds. *Marine Mammal Science* **30**, 1473-1493.
- 825 Leduc RG, Archer FI, Lang AR, Martien KK, Hancock-Hanser B, Torres-Florez JP, . . .  
826 Taylor BL (2016) Genetic variation in blue whales in the eastern pacific:  
827 implication for taxonomy and use of common wintering grounds. *Molecular*  
828 *Ecology*.
- 829 Leigh JW, Bryant D (2015) POPART: fullfeature software for haplotype network  
830 construction. *Methods in Ecology and Evolution* **6**, 1110-1116.
- 831 Li H, Durbin R (2011) Inference of human population history from individual whole-  
832 genome sequences. *Nature* **475**, 493-496.
- 833 Lyrholm T, Gyllensten U (1998) Global matrilineal population structure in sperm whales  
834 as indicated by mitochondrial DNA sequences. *Proceedings of the Royal Society*  
835 *B-Biological Sciences* **265**, 1679-1684.
- 836 Lyrholm T, Leimar O, Gyllensten U (1996) Low diversity and biased substitution  
837 patterns in the mitochondrial DNA control region of sperm whales: implications  
838 for estimates of time since common ancestry. *Molecular Biology and Evolution*  
839 **13**, 1318-1326.
- 840 Lyrholm T, Leimar O, Johannesson B, Gyllensten U (1999) Sex-biased dispersal in sperm  
841 whales: contrasting mitochondrial and nuclear genetic structure of global  
842 populations. *Proceedings of the Royal Society B-Biological Sciences* **266**, 347-  
843 354.
- 844 Martien KK, Chivers SJ, Baird RW, Archer FI, Gorgone AM, Hancock-Hanser BL, . . .  
845 Taylor BL (2014) Nuclear and mitochondrial patterns of population structure in  
846 north pacific false killer whales (*Pseudorca crassidens*). *Journal of Heredity* **105**,  
847 611-626.
- 848 Mate BR, Stafford KM, Ljungblad DK (1994) A change in sperm whale (*Physeter*  
849 *macrocephalus*) distribution correlated to seismic surveys in the Gulf of Mexico.  
850 *Journal of the Acoustical Society of America* **96**, 3268-3269.
- 851 Matzke NJ (2012) Founder-event speciation in BioGeoBEARS package dramatically  
852 improves likelihoods and alters parameter inference in Dispersal-Extinction-  
853 Cladogenesis (DEC) analyses. *Frontiers of Biogeography* **4(suppl. 1)**, 210.
- 854 Matzke NJ (2013) *BioGeoBEARS: BioGeography with Bayesian (and Likelihood)*  
855 *Evolutionary Analysis in R Scripts*, University of California, Berkeley.
- 856 Matzke NJ (2014) Model selection in historical biogeography reveals that founder-event  
857 speciation is a crucial process in island clades. *Systematic Biology* **63**, 951-970.
- 858 Mazet O, Rodriguez W, Chikhi L (2015) Demographic inference using genetic data from  
859 a single individual: Separating population size variation from population  
860 structure. *Theoretical Population Biology* **104**, 46-58.
- 861 Mazet O, Rodriguez W, Grusea S, Boitard S, Chikhi L (2016) On the importance of  
862 being structured: instantaneous coalescence rates and human evolution--lessons  
863 for ancestral population size inference? *Heredity (Edinb)* **116**, 362-371.
- 864 McGowen MR, Spaulding M, Gatesy J (2009) Divergence date estimation and a  
865 comprehensive molecular tree of extant cetaceans. *Molecular Phylogenetics and*  
866 *Evolution* **53**, 891-906.

- 867 Mesnick S, Taylor B, Archer EI, Martien K, Escorza Treviño S, Hancock-Hanser BL, . . .  
868 Morin PA (2011) Sperm whale population structure in the eastern North Pacific  
869 inferred by the use of single nucleotide polymorphisms (SNPs), microsatellites  
870 and mitochondrial DNA. *Molecular Ecology Resources* **11** (suppl. 1), 278-298.
- 871 Miller SA, Dykes DD, Polesky HF (1988) A simple salting out procedure for extracting  
872 DNA from human nucleated cells. *Nucleic Acids Research* **16**, 1215.
- 873 Mizroch SA, Rice DW (2013) Ocean nomads: Distribution and movements of sperm  
874 whales in the North Pacific shown by whaling data and Discovery marks. *Marine*  
875 *Mammal Science* **29**, E136-E165.
- 876 Morin PA, Archer FI, Foote AD, Vilstrup J, Allen EE, Wade P, . . . Harkins T (2010)  
877 Complete mitochondrial genome phylogeographic analysis of killer whales  
878 (*Orcinus orca*) indicates multiple species. *Genome Research* **20**, 908-916.
- 879 Morin PA, Parsons KM, Archer FI, Ávila-Arcos MC, Barrett-Lennard LG, Dalla Rosa L,  
880 . . . Foote AD (2015) Geographic and temporal dynamics of a global radiation and  
881 diversification in the killer whale. *Molecular Ecology* **24**, 3964-3979.
- 882 Moyle RG, Oliveros CH, Andersen MJ, Hosner PA, Benz BW, Manthey JD, . . .  
883 Faircloth BC (2016) Tectonic collision and uplift of Wallacea triggered the global  
884 songbird radiation. *Nature Communications* **7**, 12709.
- 885 Murrell B, Moola S, Mabona A, Weighill T, Sheward D, Kosakovsky Pond SL, Scheffler  
886 K (2013) FUBAR: a fast, unconstrained bayesian approximation for inferring  
887 selection. *Molecular Biology and Evolution* **30**, 1196-1205.
- 888 Murrell B, Wertheim JO, Moola S, Weighill T, Scheffler K, Kosakovsky Pond SL (2012)  
889 Detecting individual sites subject to episodic diversifying selection. *PLoS*  
890 *Genetics* **8**, e1002764.
- 891 Notarbartolo-Di-Sciara G (2014) Sperm whales, *Physeter macrocephalus*, in the  
892 Mediterranean Sea: a summary of status, threats, and conservation  
893 recommendations. *Aquatic Conservation-Marine and Freshwater Ecosystems* **24**,  
894 4-10.
- 895 Nylander JA, Wilgenbusch JC, Warren DL, Swofford DL (2008) AWTY (are we there  
896 yet?): a system for graphical exploration of MCMC convergence in Bayesian  
897 phylogenetics. *Bioinformatics* **24**, 581-583.
- 898 O'Brien SJ (1994) A role for molecular genetics in biological conservation. *Proceedings*  
899 *of the National Academy of Science USA* **91**, 5748-5755.
- 900 Omasits U, Ahrens CH, Muller S, Wollscheid B (2014) Protter: interactive protein  
901 feature visualization and integration with experimental proteomic data.  
902 *Bioinformatics* **30**, 884-886.
- 903 Pecl GT, Jackson GD (2008) The potential impacts of climate change on inshore squid:  
904 biology, ecology and fisheries. *Reviews in Fish Biology and Fisheries* **18**, 373-  
905 385.
- 906 Pettersen EF, Goddard TD, Huang CC, Couch GS, Greenblatt DM, Meng EC, Ferrin TE  
907 (2004) UCSF Chimera--a visualization system for exploratory research and  
908 analysis. *Journal of Computational Chemistry* **25**, 1605-1612.
- 909 Pimiento C, Griffin JN, Clements CF, Silvestro D, Varela S, Uhen MD, Jaramillo C  
910 (2017) The Pliocene marine megafauna extinction and its impact on functional  
911 diversity. *Nat Ecol Evol* **1**, 1100-1106.

- 912 Pond SL, Frost SD (2005) Datamonkey: rapid detection of selective pressure on  
913 individual sites of codon alignments. *Bioinformatics* **21**, 2531-2533.
- 914 Pond SL, Frost SD, Muse SV (2005) HyPhy: hypothesis testing using phylogenies.  
915 *Bioinformatics* **21**, 676-679.
- 916 Premo LS, Hublin JJ (2009) Culture, population structure, and low genetic diversity in  
917 Pleistocene hominins. *Proc Natl Acad Sci U S A* **106**, 33-37.
- 918 R Core Team (2014) R: A language and environment for statistical computing. R  
919 Foundation for Statistical Computing, Vienna, Austria. [https://www.R-](https://www.R-project.org)  
920 [project.org](https://www.R-project.org).
- 921 Rambaut A, Suchard MA, Xie D, Drummond AJ (2014) Tracer v1.6.  
922 <http://tree.bio.ed.ac.uk/software/tracer/>.
- 923 Ready J, Kaschner K, South AB, Eastwood PD, Rees T, Rius J, . . . Froese R (2010)  
924 Predicting the distributions of marine organisms at the global scale. *Ecological*  
925 *Modelling* **221**, 467-478.
- 926 Saier MH (1994) Computer-aided analyses of transport protein sequences: gleanings  
927 evidence concerning function, structure, biogenesis, and evolution.  
928 *Microbiological Reviews* **58**, 71-93.
- 929 Sambrook J, Fritsch EF, Maniatis T (1989) *Molecular Cloning: A Laboratory Manual*,  
930 2nd edn. Cold Spring Harbor Laboratory Press, Cold Spring Harbor, New York.
- 931 Savery LC, Wise JT, Wise SS, Falank C, Gianios C, Jr., Thompson WD, . . . Wise JP, Sr.  
932 (2014a) Global assessment of arsenic pollution using sperm whales (*Physeter*  
933 *macrocephalus*) as an emerging aquatic model organism. *Comparative*  
934 *Biochemistry and Physiology. Toxicology and Pharmacology*. **163**, 55-63.
- 935 Savery LC, Wise SS, Falank C, Wise J, Gianios C, Jr., Douglas Thompson W, . . . Wise  
936 JP, Sr. (2014b) Global assessment of oceanic lead pollution using sperm whales  
937 (*Physeter macrocephalus*) as an indicator species. *Marine Pollution Bulletin* **79**,  
938 236-244.
- 939 Schwede T, Kopp J, Guex N, Peitsch MC (2003) SWISS-MODEL: An automated protein  
940 homology-modeling server. *Nucleic Acids Research* **31**, 3381-3385.
- 941 Shamblin BM, Bjorndal KA, Bolten AB, Hillis-Starr ZM, Lundgren I, Naro-Maciel E,  
942 Nairn CJ (2012) Mitogenomic sequences better resolve stock structure of southern  
943 Greater Caribbean green turtle rookeries. *Molecular Ecology* **21**, 2330-2340.
- 944 Somero GN (1992) Biochemical ecology of deep-sea animals. *Experientia* **48**, 537-543.
- 945 Steiner L, Lamoni L, Plata MA, Jensen SK, Lettevall E, Gordon J (2012) A link between  
946 male sperm whales, *Physeter macrocephalus*, of the Azores and Norway. *Journal*  
947 *of the Marine Biological Association of the United Kingdom* **92**, 1751-1756.
- 948 Straley JM, Schorr GS, Thode AM, Calambokidis J, Lunsford CR, Chenoweth EM, . . .  
949 Andrews RD (2014) Depredating sperm whales in the Gulf of Alaska: local  
950 habitat use and long distance movements across putative population boundaries.  
951 *Endangered Species Research* **24**, 125-135.
- 952 Tamura K, Stecher G, Peterson D, Filipinski A, Kumar S (2013) MEGA6: Molecular  
953 Evolutionary Genetics Analysis version 6.0. *Molecular Biology and Evolution* **30**,  
954 2725-2729.
- 955 Taylor BL, Chivers SJ, Larese J, Perrin WF (2007) Generation length and percent mature  
956 estimates for IUCN assessments of cetaceans. Administrative Report, Southwest  
957 Fisheries Science Center, 8604 La Jolla Shores Blvd., La Jolla, CA 92038, USA.

- 958 Tiedemann R, Milinkovitch MC (1999) Culture and genetic evolution in whales. *Science*  
959 **284**, 2055a.
- 960 Unger B, Rebolledo EL, Deaville R, Grone A, LL IJ, Leopold MF, . . . Herr H (2016)  
961 Large amounts of marine debris found in sperm whales stranded along the North  
962 Sea coast in early 2016. *Marine Pollution Bulletin* **112**, 134-141.
- 963 Van Cise A, Morin PA, Baird RW, Lang AR, Robertson KM, Chivers SJ, . . . Martien  
964 KK (2016) Redrawing the map: mtDNA provides new insights into the  
965 distribution and diversity of short-finned pilot whales in the Pacific Ocean.  
966 *Marine Mammal Science* **32**, 1177-1199.
- 967 Warren DL, Geneva AJ, Lanfear R (2017a) RWTY (R We There Yet): An R package for  
968 examining convergence of Bayesian phylogenetic analyses. *Molecular Biology*  
969 *and Evolution* **34**, 1016-1020.
- 970 Warren WC, Kuderna L, Alexander A, Catchen J, Pérez-Silva JG, López-Otín C, . . .  
971 Wise Sr. JP (2017b) The novel evolution of the sperm whale genome. *Genome*  
972 *Biology and Evolution* **9**, 3260-3264.
- 973 Whitehead H (1998) Cultural selection and genetic diversity in matrilineal whales.  
974 *Science* **282**, 1708-1711.
- 975 Whitehead H (2002) Estimates of the current global population size and historical  
976 trajectory for sperm whales. *Marine Ecology Progress Series* **242**, 295-304.
- 977 Whitehead H (2005) Genetic diversity in the matrilineal whales: Models of cultural  
978 hitchhiking and group-specific non-heritable demographic variation. *Marine*  
979 *Mammal Science* **21**, 58-79.
- 980 Whitehead H, Vachon F, Frasier TR (2017) Cultural hitchhiking in the matrilineal  
981 whales. *Behavior Genetics* **47**, 324-334.
- 982 Wilgenbusch JC, Warren DL, Swofford DL (2004) AWTY: a system for graphical  
983 exploration of MCMC convergence in Bayesian phylogenetic inference.  
984 [http://king2.sc.fsu.edu/CEBProjects/awty/awty\\_start.php](http://king2.sc.fsu.edu/CEBProjects/awty/awty_start.php).
- 985 Woolley S, Johnson J, Smith MJ, Crandall KA, McClellan DA (2003) TreeSAAP:  
986 selection on amino acid properties using phylogenetic trees. *Bioinformatics* **19**,  
987 671-672.
- 988 Yang Z (2007) PAML 4: phylogenetic analysis by maximum likelihood. *Molecular*  
989 *Biology and Evolution* **24**, 1586-1591.
- 990 Yang Z, Wong WS, Nielsen R (2005) Bayes empirical bayes inference of amino acid  
991 sites under positive selection. *Molecular Biology and Evolution* **22**, 1107-1118.  
992

993 **Data Accessibility**

994

995 Mitogenome haplotype sequences generated for this study have been submitted to  
996 GenBank (accession numbers KU891329 - KU891394). Sequence alignment input and  
997 output xml file from Beast phylogenetic and skyline/skygrid analyses are available from  
998 the Dryad Digital Repository doi:10.5061/dryad.57271.

999

1000 **Author Contributions**

1001

1002 PAM and SLM conceived of the study. CSB, BRM, SLM, HW, KK, PER and AA  
1003 contributed samples, data, and expert interpretation. BLH, VLP and AA generated  
1004 genetic data. PAM, AA and ADF conducted analyses and wrote the manuscript.

1005

1006

1007 **Figures legends**

1008

1009 Figure 1. Map of all samples used in this study. Black circles = new mitogenome data,  
1010 gray triangles = previously published mitogenome sequences (Alexander *et al.* 2013).  
1011

1012 Figure 2. Time-calibrated (millions of years) phylogeny of all unique sperm whale  
1013 mitochondrial genomes. Posterior probability support >0.5 is shown at nodes. Haplotype  
1014 ID's are provided as "mt###" (see supplemental Table S1 for samples associated with  
1015 haplotypes) followed by abbreviated locations (see supplemental Table S1). The clades to  
1016 the right correspond to the pruned tree clades used for phylogeographic analysis (Figure  
1017 5). Branches are color coded by ocean basin where haplotypes are found: Blue = Pacific,  
1018 Red = Atlantic, Green = Indian, Orange = Mediterranean, Pink = Pacific/Atlantic  
1019 (shared). \*Mitogenome haplotypes assembled from SRA data (Warren *et al.* 2017b).  
1020

1021 Figure 3. Median Joining Network of all unique haplotypes, colored by ocean. Tick  
1022 marks on branches indicate the number of nucleotide differences. Not all 80 unique  
1023 haplotypes are included in the network, as the algorithm collapses haplotypes with  
1024 missing or ambiguous positions.  
1025

1026 Figure 4. Demographic reconstructions based on the sperm whale mitogenomes and  
1027 nuclear genome PSMC. The mitogenome skyline (black) and skygrid (gray) plot lower  
1028 and upper 95% highest posterior density intervals are shown by thinner lines and median  
1029 values by thicker lines. Demographic estimates were converted to effective population  
1030 size (females) by dividing by a  $\tau$  of 31.9 years (Taylor *et al.* 2007). The nuclear PSMC  
1031 plots are for three sperm whales from the Atlantic (red), Pacific (blue), and Indian  
1032 (yellow) Oceans. Pseudo-diploid plots are shown for each ocean pair: Atlantic-Pacific  
1033 (green), Atlantic-Indian (pink), and Pacific-Indian (purple). The X axis starts at 10,000 yr  
1034 before present, and the Y axis is truncated at  $3.5 \times 10^4$ , as pseudo-diploid plots increase  
1035 exponentially and bootstrap variation at  $< 2 \times 10^4$  years was very large. Glacial maxima  
1036 and Eemian warm period are shown with beige and yellow shading, respectively.  
1037 Bootstrap plots for each PSMC analysis are presented in supplemental Figure S1.  
1038

1039 Figure 5. Most probable ancestral ranges for sperm whale populations estimated using the  
1040 best fit model DEC+J from BioGeoBEARS and full mitogenomes. Clade IDs (tips) are as  
1041 in Figure 2, and represent the tree topology pruned to one tip per clade. The boxes at  
1042 nodes indicate the most likely geographic range immediately after cladogenesis. Oceanic  
1043 regions are indicated by P = Pacific, A = Atlantic, I = Indian, M = Mediterranean.  
1044

1045 Figure 6. AquaMaps environmental envelope models for distribution of female sperm  
1046 whale habitat mapped to environmental conditions for a) last glacial maximum and b)  
1047 current habitat. Dark red color indicates core suitable habitat; yellow indicates marginal  
1048 habitat.  
1049

Table 1  
Number of haplotypes, haplotypic diversity and nucleotide diversity by ocean basin.

	No. Samples	No. Haplotypes	Haplotype Diversity	Nucleotide Diversity ( $\pi$ )
Atlantic*	35	10	0.839	0.000991
GoMx	11	5	0.818	0.001019
Mediterranean	4	2	0.500	0.000000
Pacific	124	66	0.972	0.000795
Global†	175	80	0.975	0.000934

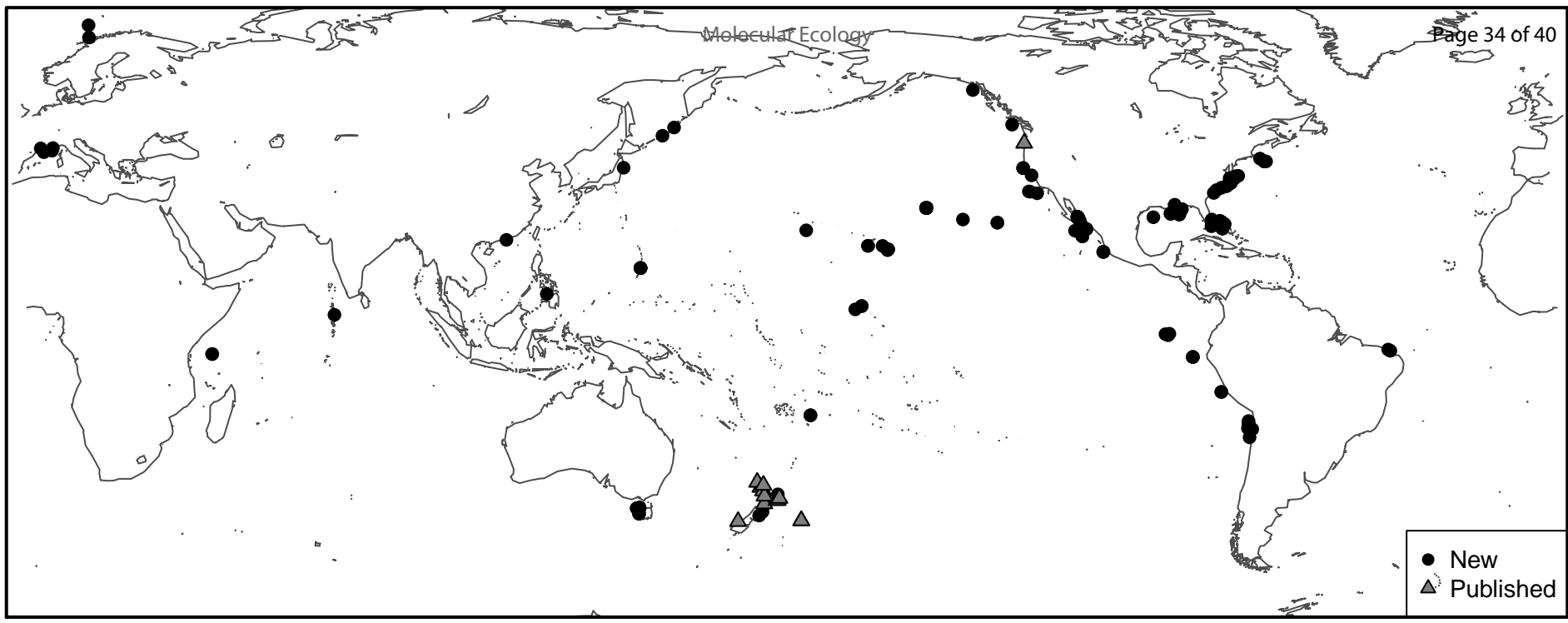
\*excluding the Gulf of Mexico and Mediterranean Sea.

†includes single sample from the Indian Ocean.

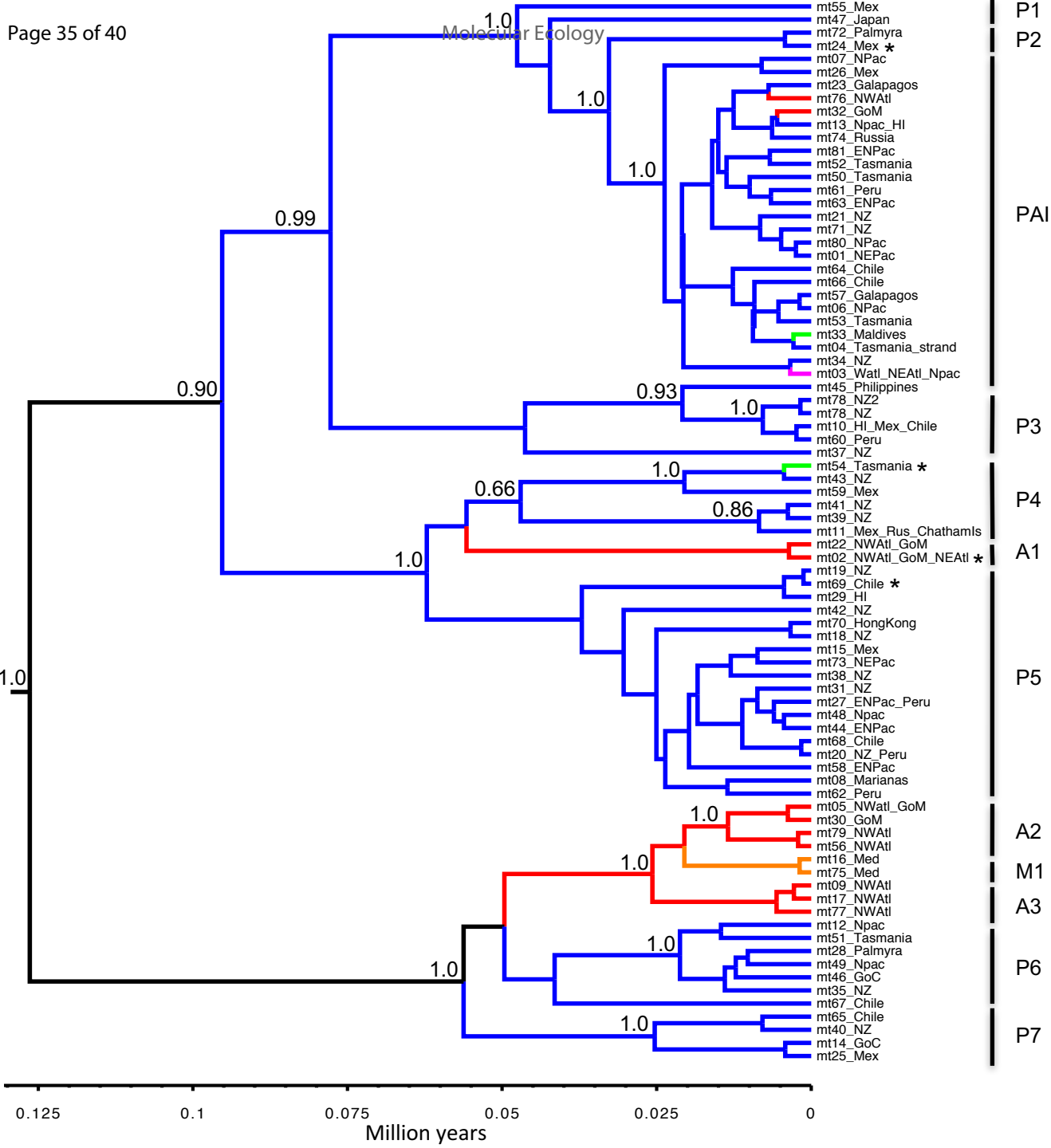
Table 2

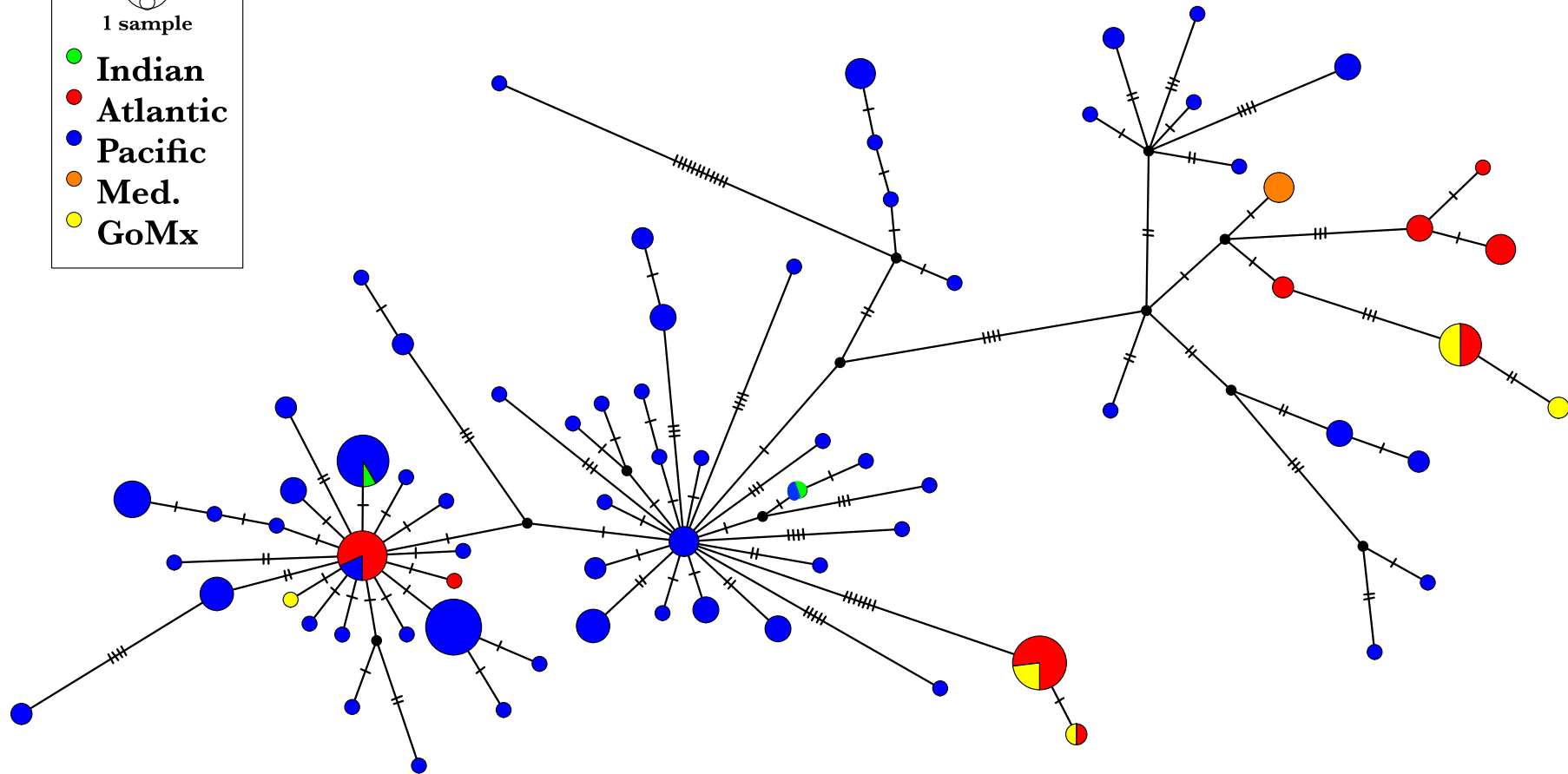
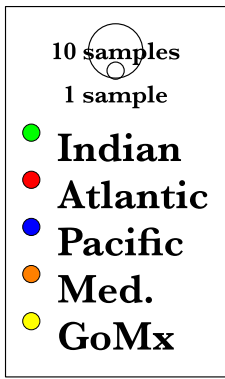
Random forest assignment of samples to ocean basin, percent correctly assigned, and lower (LCI) and upper (UCI) 95% confidence limits. All sample origins were known (rows), but assigned to ocean basins based on the training subset of mitogenomes.

	Atlantic	Pacific	pct correct	LCI	UCI
Atlantic	39	11	78	64.0	88.5
Pacific	0	124	100	97.1	100

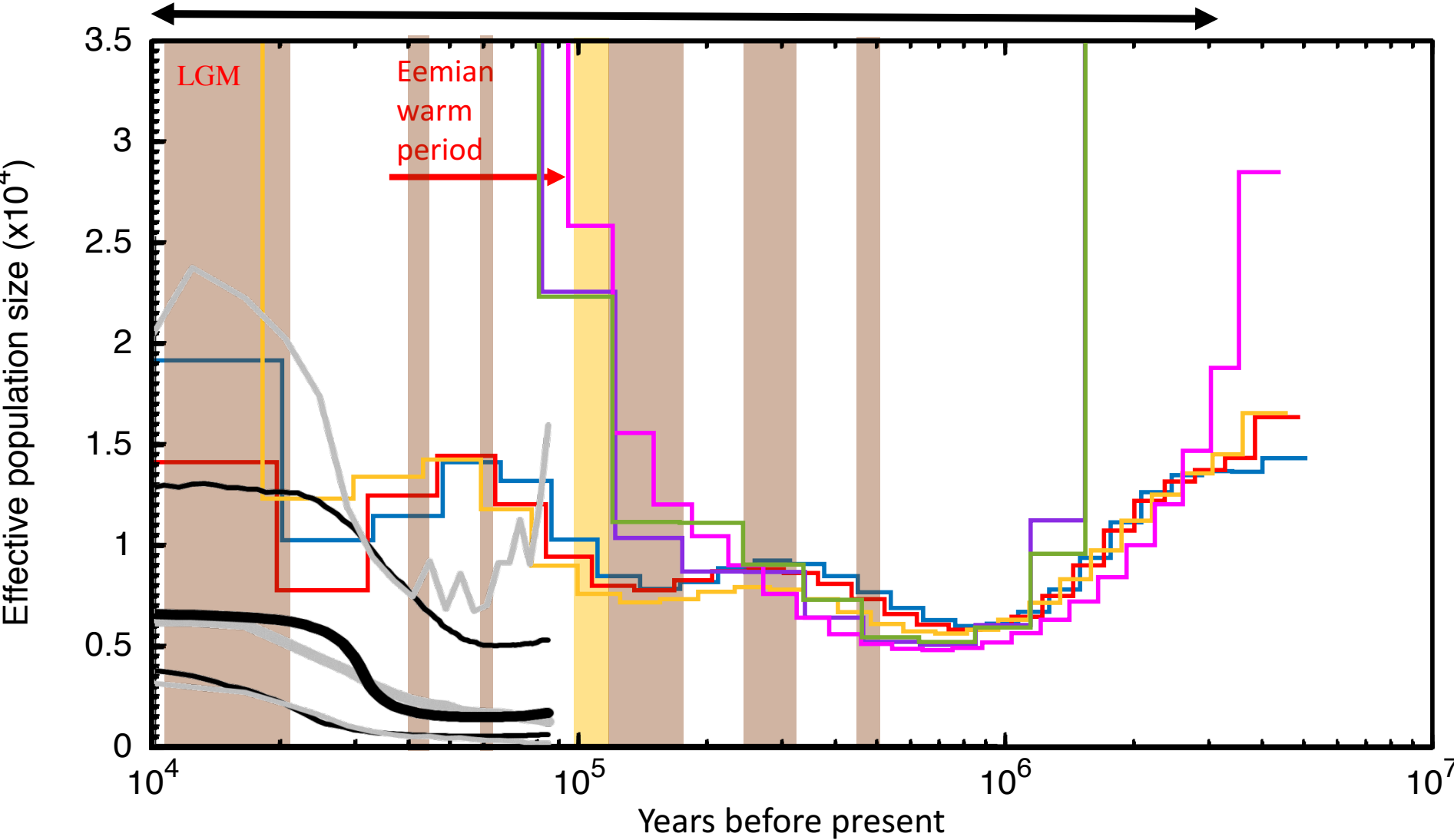


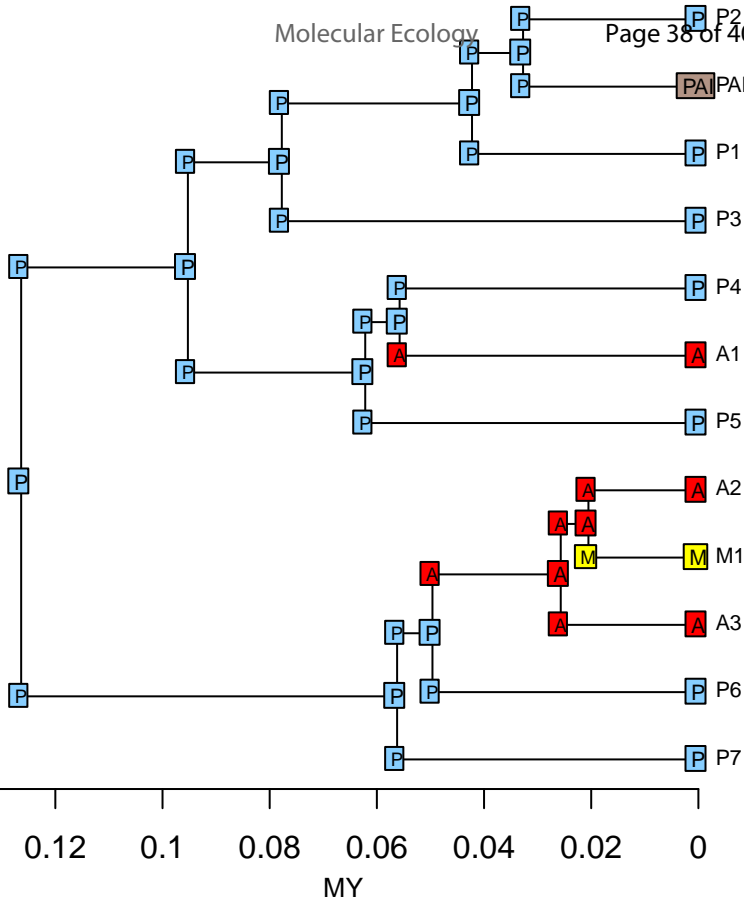
Molecular Ecology





# "ice-house" Molecular Ecology





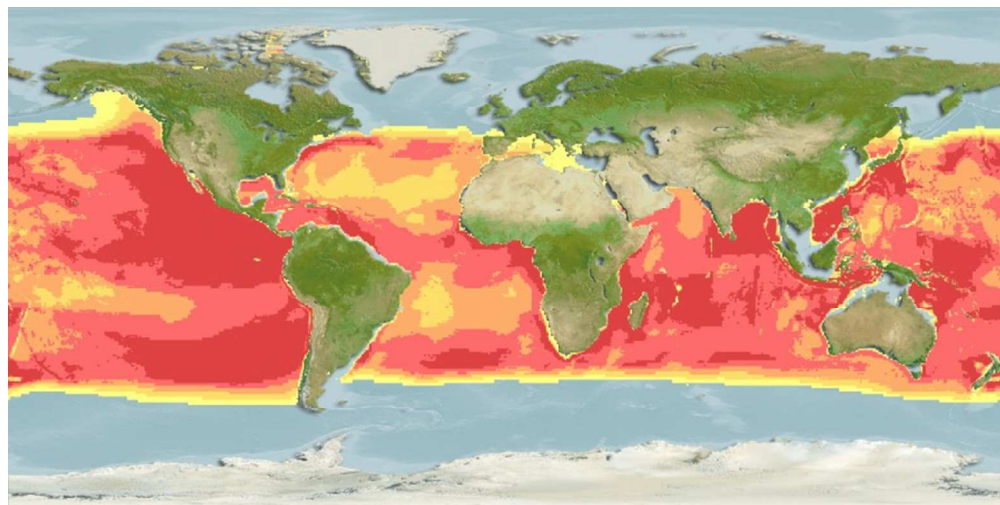
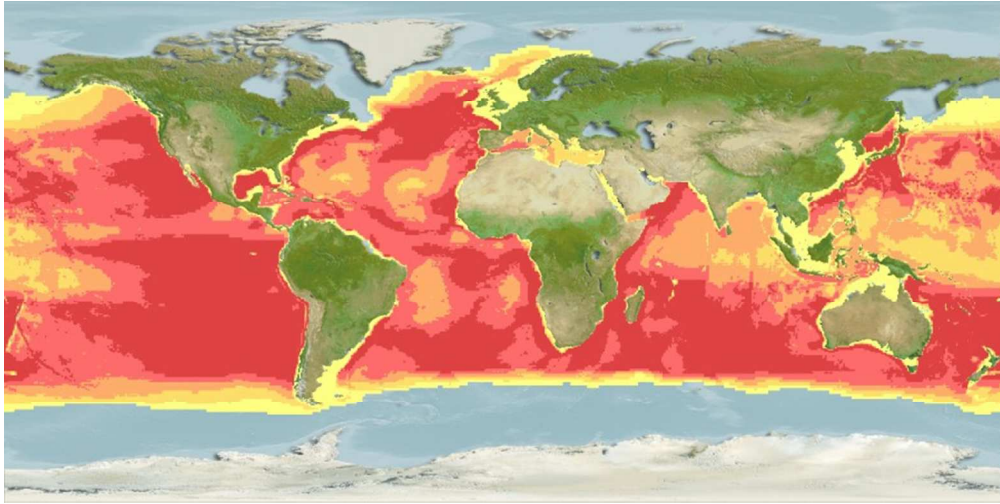


Figure 6. AquaMaps environmental envelope models for distribution of female sperm whale habitat mapped to environmental conditions for a) last glacial maximum and b) current habitat. Dark red color indicates core suitable habitat; yellow indicates marginal habitat.

317x158mm (72 x 72 DPI)



317x158mm (72 x 72 DPI)